NATIONAL AERONAUTICS AND SPACE ADMINISTRATION

Technical Report 32-1505
Supplement 1

Satellite Auxiliary-Propulsion Selection Techniques

Application of Selection Techniques to the ATS-H Satellite

Lee B. Holcomb

JET PROPULSION LABORATORY
CALIFORNIA INSTITUTE OF TECHNOLOGY
PASADENA, CALIFORNIA

October 1, 1972

N72-33867

TECHNICAL REPORT STANDARD TITLE PAGE

1. Report No. 32-1505 Supplement 1	2. Government Accession No.	3. Recipient's Catalog No.
4. Title and Subtitle SATELLITE AUXILIARY-PROPULSION SELECTION TECHNIQUES APPLICATION OF SELECTION TECHNIQUES TO THE ATS-H SATELLITE		5. Report Date October 1, 1972
		6. Performing Organization Code
7. Author(s) Lee B. Holcomb		8. Performing Organization Report No.
9. Performing Organization Name and Address JET PROPULSION LABORATORY California Institute of Technology 4800 Oak Grove Drive Pasadena, California 91103		10. Work Unit No.
		11. Contract or Grant No. NAS 7-100
		13. Type of Report and Period Covered Technical Report
12. Sponsoring Agency Name and Address NATIONAL AERONAUTICS AND SPACE ADMINISTRATION Washington, D.C. 20546		14. Sponsoring Agency Code
15. Supplementary Notes		

16. Abstract

Jet Propulsion Laboratory Technical Report 32-1505 and the addendum thereto described auxiliary-propulsion systems applicable to unmanned satellites and documented an approach for satellite designers to use in selecting systems which are the most effective for their missions. This supplement discusses the analysis required to estimate auxiliary-propulsion system requirements for a mission which includes tipoff rate reduction, acquisitions, disturbance torques, orbital disturbances, and spacecraft commanded maneuvers. The comparison of several candidate auxiliary-propulsion systems and system combinations for an Advanced Applications Technology Satellite (ATS-H) is described. A generalized auxiliary-propulsion system tradeoff, based on mission cost effectiveness criteria, is presented. The specific mission assumptions for the ATS-H spacecraft are included, along with a discussion of the sensitivity of the final selection to these assumptions.

17. Key Words (Selected by Author(s)) Control and Guidance Propulsion, Electric Propulsion, Liquid Applications Technology Satellites	18. Distribution Statement Unclassified -- Unlimited

19. Security Classif. (of this report)	20. Security Classif. (of this page)	21. No. of Pages	22. Price
Unclassified	Unclassified	30	

Preface

The work described in this report was sponsored by the Applications Technology Satellites Program Office of the NASA Office of Applications and was performed by the Propulsion Division of the Jet Propulsion Laboratory.

Acknowledgment

Many corporations and government agencies provided photographs, data, and supplementary information for this report. The author thanks them for this assistance. The author particularly acknowledges the cooperation of H. Raymond and W. J. Guman of Fairchild Hiller, R. E. Alexovich of NASA Lewis Research Center, R. C. McElvain and L. Gould of Hughes Aircraft Company, and J. Hyman Jr., J. Molitor, and W. Herron of Hughes Research Laboratories. Special thanks are due J. H. Kelley, P. I. Moynihan, and D. J. Kerrisk of JPL for continuing assistance in completing the work described herein.

NATIONAL AERONAUTICS AND SPACE ADMINISTRATION

Technical Report 32-1505

Supplement 1

Satellite Auxiliary-Propulsion Selection Techniques

Application of Selection Techniques to the ATS-H Satellite

Lee B. Holcomb

JET PROPULSION LABORATORY
CALIFORNIA INSTITUTE OF TECHNOLOGY
PASADENA, CALIFORNIA

October 1, 1972

Prepared Under Contract No. NAS 7-100
National Aeronautics and Space Administration

Contents

Contents (contd)

Tables

Figures

Contents (contd)

Figures (contd)

Abstract

Jet Propulsion Laboratory Technical Report 32-1505 and the addendum thereto described auxiliary-propulsion systems applicable to unmanned satellites and documented an approach for satellite designers to use in selecting systems which are the most effective for their missions. This supplement discusses the analysis required to estimate auxiliary-propulsion system requirements for a mission which includes tipoff rate reduction, acquisitions, disturbance torques, orbital disturbances, and spacecraft commanded maneuvers. The comparison of several candidate auxiliary-propulsion systems and system combinations for an Advanced Applications Technology Satellite (ATS-H) is described. A generalized auxiliary-propulsion system tradeoff, based on mission cost effectiveness criteria, is presented. The specific mission assumptions for the ATS-H spacecraft are included, along with a discussion of the sensitivity of the final selection to these assumptions.

Satellite Auxiliary-Propulsion Selection Techniques

Application of Selection Techniques to the ATS-H Satellite

I. Introduction

This supplement presents a comparison of several auxiliary-propulsion systems for an Advanced Applications Technology Satellite (ATS-H) and is intended to serve as an example of the auxiliary-propulsion selection techniques developed at the Jet Propulsion Laboratory and presented in Ref. 1. The chemical and electrical auxiliary-propulsion system data presented in the primary document (Ref. 1) and the addendum thereto (Ref. 2) are brought together in this example system comparison.

Several aspects of auxiliary-propulsion system selection not discussed in detail in Ref. 1 are addressed in this supplement. These include the methods used for the approximation of spacecraft disturbance torques and their associated propulsion requirements, along with the equations and data necessary to compute the propulsion requirements for tipoff rate reduction, acquisition, commanded turns, north–south stationkeeping, east–west stationkeeping, solar pressure orbit perturbations, and station changing. In addition, the sensitivity of system comparisons to mission assumptions is presented and discussed in detail.

Five candidate system options are compared:

- Option I. A monopropellant hydrazine system.
- Option II. An ion bombardment system with an inert gas system.
- Option III. A pulsed plasma system with an inert gas system.
- Option IV. A pulsed plasma system with a hydrazine system.
- Option V. An ion bombardment system with a hydrazine system.

This list includes both chemical and electric propulsion systems. Options II and III have small inert gas systems (required for a few relatively high torque maneuvers) coupled with auxiliary electric propulsion systems. The electric propulsion systems will perform all other spacecraft propulsive functions. Options IV and V have hydrazine systems coupled with the auxiliary electric propulsion systems. The hydrazine systems will perform the high torque maneuvers and the other attitude propulsion functions, whereas the auxiliary electric propulsion systems will perform north–south stationkeeping, east–west stationkeeping, and low-thrust station changes.

The ATS-H spacecraft was chosen for this study for several reasons. First, the experiments on the ATS-H spacecraft require high power; therefore this spacecraft has electrical power which can be shared with the electric propulsion options. In addition, lightweight solar arrays will be used for electric power, reducing the specific mass penalty for power and making the ATS-H spacecraft attractive for the application of auxiliary electric propulsion systems. Since the ATS-H spacecraft is still under study, it is possible to freely substitute different propulsion system options during the early design stages. Once a space program is proposed by NASA for a given cost and committed to by the Office of Management and Budget and Congress at that cost, changes in the spacecraft or its subsystems (e.g., changes which decrease spacecraft mass at increased cost or increase spacecraft reliability at increased cost) are strongly constrained by the "fixed" program cost. There is also an overwhelming reluctance on the part of subsystem hardware designers to regress to a less reliable or less costly design option to provide additional funds or mass for other subsystems—even though such a change or reallocation could be shown to benefit the overall spacecraft design or program cost effectiveness. The greatest opportunity to optimally allocate mass, cost, and manpower resources among subsystems and to various phases of the spacecraft development occurs during preliminary design planning stages.

II. Spacecraft Objectives and Program Assumptions

The primary objective of the Advanced Applications Technology Satellite (ATS-H) is to demonstrate a high-power communications system placed in synchronous orbit above the United States. The spacecraft will be able to attain 0.1-deg antenna pointing accuracy, with a capability of broadcasting to isolated areas such as Appalachia, Alaska, and Hawaii, and will have a design life of five years. However, it is not the purpose of this report to present the spacecraft objectives.

In order to utilize the selection techniques, described in Ref. 1, program assumptions must be discussed. A total program cost of $120 million is assumed. This estimate is based on the ATS-F and -G program. The sensitivity of the selection techniques to total program cost will subsequently be demonstrated by using total program costs of $100 and $140 million.

The mission worth and probability of success are presented in Figs. 1 and 2, respectively. The magnitude of mission worth is not important to this effort. However, when looking at the final values of cost effectiveness, it is possible to assign a value to the product of worth times probability of success as being equal to total program cost. In other words, the mission effectiveness or mission usefulness is about equal to the total program cost.

The mission worth profile presented in Fig. 1 is for a spacecraft with slowly degrading performance as a function of time in orbit. Two alternative curves of mission worth are presented in Fig. 1. The sensitivity of the results to substitution of these mission worth curves will be discussed.

The mission probability of success presented in Fig. 2 is typical for a communications satellite like ATS-H. It shows relatively large gains in mission probability of success associated with increases in redundancy mass. Another mission probability of success curve is presented in Fig. 3. This curve is typical of a very complex satellite which has been designed with the knowledge that considerable redundancy must be incorporated into the satellite in order to achieve long life. Although the mission probability of success is relatively low for this spacecraft when no redundancy mass is incorporated, it will increase rather rapidly when additional mass is allocated to redundancy. As subsystems are made more reliable by the addition of redundancy, the increase in overall mission probability of success becomes smaller with the continued addition of redundancy mass (i.e., a diminishing return). The sensitivity of the results to different values of worth and probability of success is discussed in a later section using the modified mission data presented here.

III. Spacecraft Configuration

Hughes Aircraft Company and Fairchild Industries have performed mission studies of an advanced Applications Technology Satellite (Refs. 3, 4). Each contractor has selected two spacecraft configurations. One spacecraft configuration allows for raising the orbit to synchronous altitute by spiraling-out with electric propulsion; the other allows for direct synchronous orbit insertion by a solid-propellant apogee motor. A spacecraft mass of 680 kg in synchronous orbit was selected.[1] A baseline spacecraft mass of 453 kg is assumed, with an additional

[1]Throughout this report the International System of Units (S.I.) is used exclusively. The conversion coefficients used to convert English units to S.I. units are included in the Nomenclature.

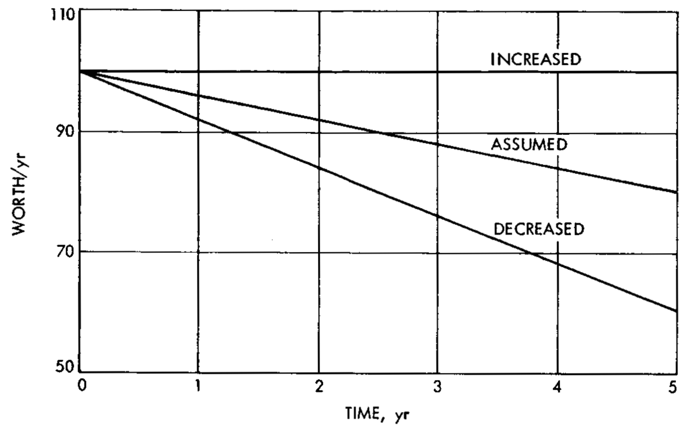

Fig. 1. Mission worth

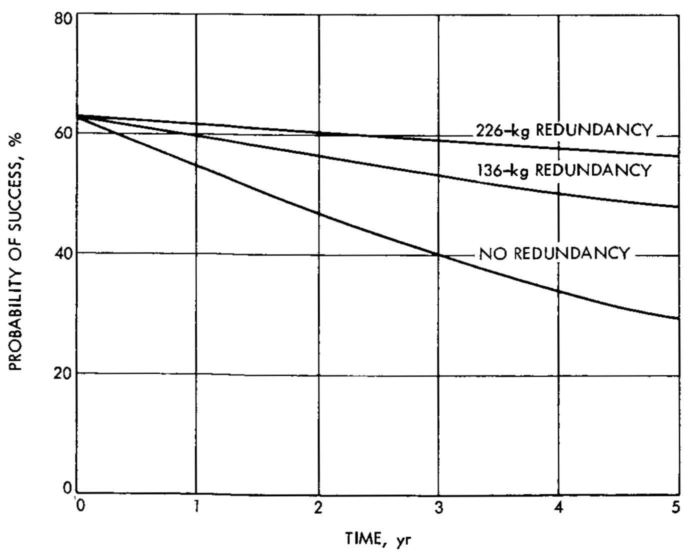

Fig. 2. Assumed mission probability of success

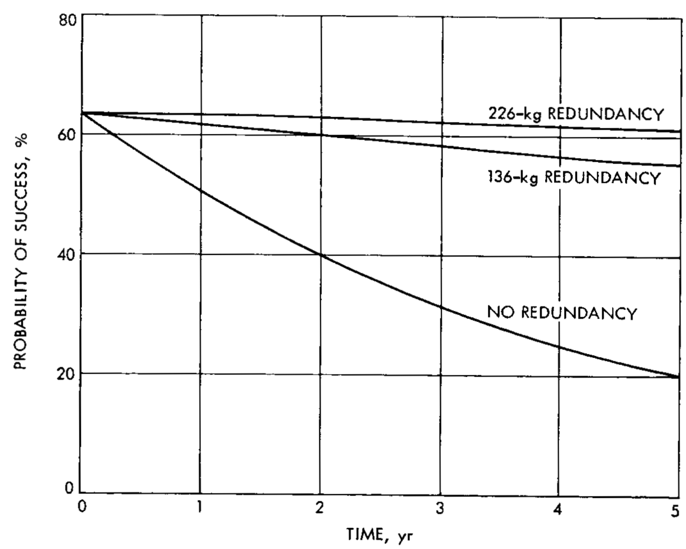

Fig. 3. Modified mission probability of success

226 kg available for allocation to spacecraft redundancy or to be added to the auxiliary propulsion system. This spacecraft mass falls between the synchronous payload of a Delta-launched, electric propulsion, spiral-out spacecraft and an Atlas/Centaur-launched, solid-propellant, apogee motor spacecraft. The method of orbit insertion is not discussed here. The Hughes "A" spacecraft configuration, which allows for electric propulsion spiral-out to synchronous orbit, was selected for the purpose of this study.

During the electric propulsion spiral-out to synchronous orbit (approximately 60–90 days), the solar panel axis is oriented in the north–south direction (Fig. 4). Once the proper synchronous orbit has been achieved, the spacecraft is rotated to align the solar panel axis in the east–west direction (Fig. 5). During the spiral-out phase, the solar panels are oriented toward the sun, while the spacecraft body and antenna are pointed toward the earth. Once on station, the solar panels and body are oriented toward the sun, while the antenna is pointed toward the earth. Therefore, two rotating connections are required—one for the solar panel/body interface, the other for the antenna/body interface. This spacecraft could be placed directly into synchronous orbit by a solid-propellant apogee rocket engine and oriented with the solar panels in an east–west direction. This mode of orbit insertion would require only one spacecraft rotation connection between the spacecraft body and antenna. The spacecraft solar panels were sized for electric propulsion orbit-raising mission. This makes the attitude propulsion requirements slightly larger than expected for the direct orbit insertion mission because of the resulting higher solar pressure torques.

The Hughes "A" configuration is depicted in Fig. 6. This figure includes the referenced axes and spacecraft dimensions. The center of solar pressure and center-of-gravity offset are assumed to be 0.23 m in axis 3 and 0.03 m in axes 1 and 2. After spacecraft launch and prior to solar panel deployment, the spacecraft moments of inertia are 840 N-m-s^2 about axis 1 and 1085 N-m-s^2 about axes 2 and 3. With solar panel deployment, the spacecraft moments of inertia are 840 N-m-s^2 about axis 1, 14,446 N-m-s^2 about axis 2, and 14,056 N-m-s^2 about axis 3.

Since it is the intention of this report to select the optimum auxiliary propulsion system, the attitude control system will not be described in great detail and the justification for any components that are discussed will not be given. In general, the attitude control system is comprised of coarse and fine sun sensors along with earth sensors; it may or may not include a Polaris sensor. The system is assumed to include very low drift (0.001 deg/h) rate integrating gyros of the gas-bearing type. Gyro drift corrections are transmitted from earth appoximately twice a day based on telemetry data from the sun and celestial sensors and the gyro output. The gyro system could be removed and a Polaris sensor used for three-axes reference; however, the output from the gyro system is easily substituted as a celestial reference. An active system is required to maintain the spacecraft position in space. One single "biased" momentum wheel could be used, but the selected system for this study is three small reaction wheels. In several of the comparisons these reaction wheels will be replaced by pulsed plasma thrusters operating in a limit cycle mode. The small reaction wheels are sized according to disturbance torques experienced in space and must be "unloaded" several times a day. This requires the firing of an appropriate thruster to generate a counter torque during reaction wheel desaturation. It is assumed that the reaction wheels can generate sufficient torque to position the spacecraft and that the flexibility of the solar panels can be handled. Studies at JPL have indicated that the torque levels of the pulsed plasma thrusters (described later herein) are also high enough to handle solar panel flexibility (Ref. 5).

Although five system options were described in Section I, only four basic propulsion types are represented (catalytic monopropellant hydrazine, inert gas, ion bombardment, and pulsed plasma). Each of these four propulsion types will be configured as shown in Figs. 7 and 8. The basic functions these systems must perform are:

(1) Spacecraft tip-off rate reduction.

(2) Acquisition of references.

(3) Reaction wheel desaturation or limit cycle operation.

(4) Commanded or unusual incident maneuvers.

(5) North–south stationkeeping.

(6) East–west stationkeeping.

(7) Orbit correction due to solar pressure perturbations.

(8) Spacecraft ΔV for positioning or station change.

Functions 1 through 4 require thrusters to provide roll, pitch, and yaw torque. A matrix of the desired thruster actuation for the proper function can be generated from the thruster designations of Figs. 7 and 8. The correct

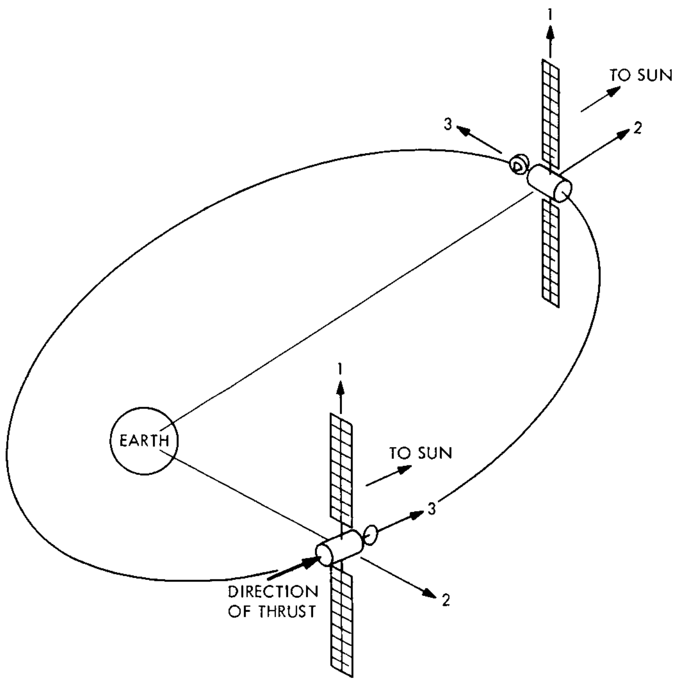

Fig. 4. Spiral-out spacecraft orientation

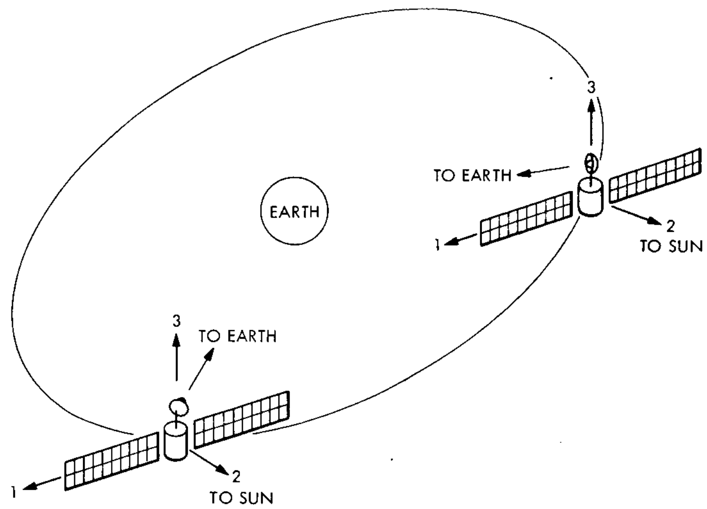

Fig. 5. On-station spacecraft orientation

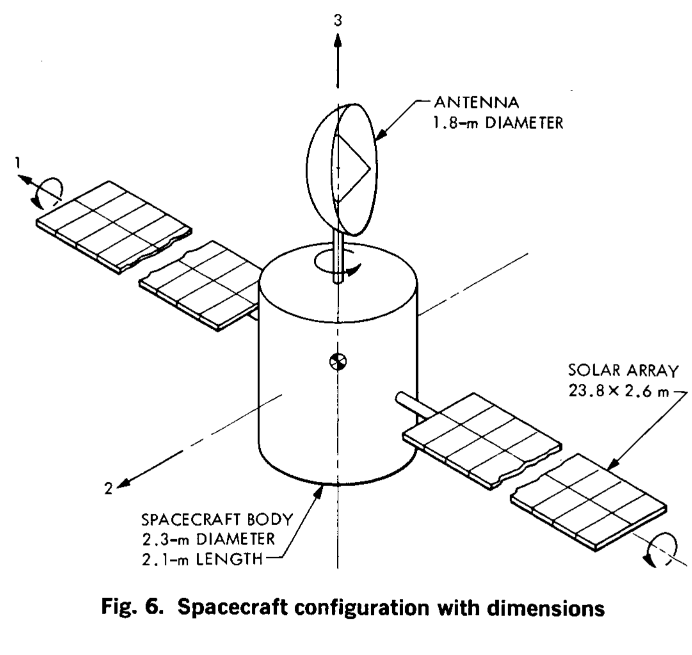

Fig. 6. Spacecraft configuration with dimensions

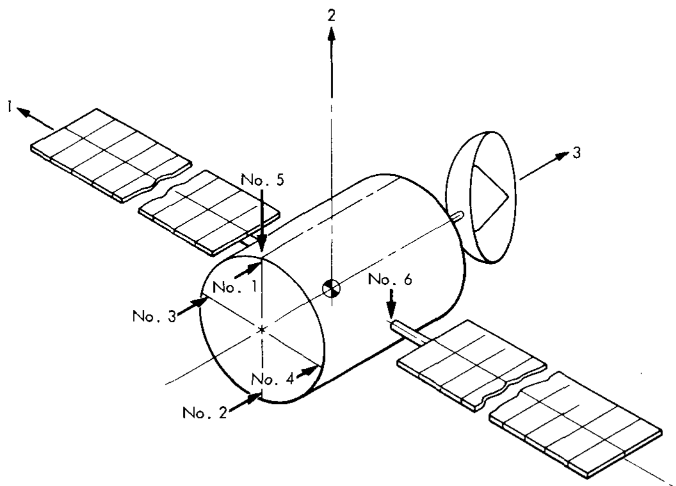

Fig. 7. Thruster locations for the inert gas, hydrazine, and pulsed plasma systems

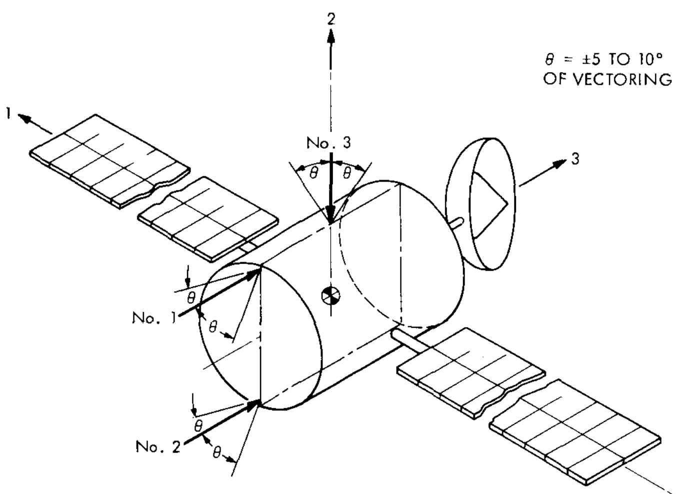

Fig. 8. Thruster locations for ion bombardment systems

thruster firings for functions 1 to 4, which require torques, can be selected from Table 1. Noncoupled thruster actuation will result in the generation of a spacecraft torque along with spacecraft translation. The torque levels of each of these thruster orientations are also given and will be referenced subsequently.

The north–south stationkeeping function must be performed at specific times during the orbit to obtain the maximum efficiency from thrusters. The best time for thruster actuation occurs at the node points of the orbit. These points are shown in Fig. 9. For a spacecraft with its north–south thrusters located as in Figs. 7 and 8, there exists only one period per day when the thruster should be actuated for north or south corrections. Actuation of

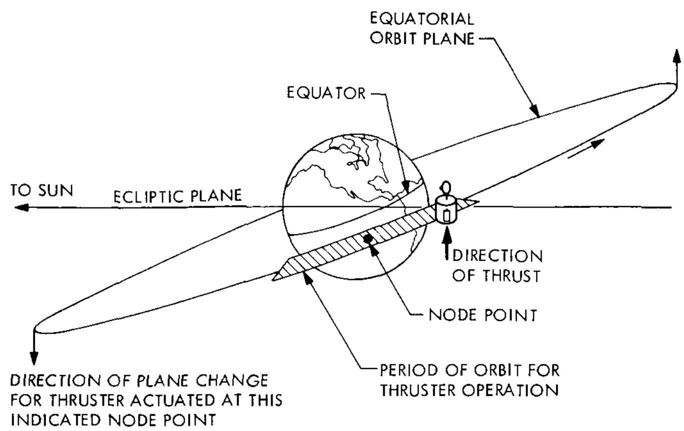

Fig. 9. Thrusting program for north–south stationkeeping

the thrusters can last up to several hours before cosine losses begin to dominate. When this occurs, operation must cease. A summary of the proper thruster actuation for north–south stationkeeping is presented in Table 2.

The east–west stationkeeping functions must also be performed at specific times during the orbit to obtain maximum effect from the thrusters. The best times for thruster actuations are shown in Fig. 10. For a spacecraft with its east–west thrusters located as in Figs. 7 and 8, thrusters should be actuated for only one period per day for either the east or west corrections. Operation of these thrusters is nominally for a short period of time (several minutes per day) since east–west orbit perturbations are small. A summary of the required thruster actuation for east–west stationkeeping functions is presented in Table 2.

Orbital corrections due to solar pressure perturbations must be performed at two specific times during the orbit to maximize the effect from the thruster. The optimum times for thruster operation are given in Fig. 11. For a spacecraft with its east–west thruster located as in Figs. 7 and 8, there exist only two periods per day when the thruster should be actuated to compensate for solar pressure orbit perturbation. A summary of the required thruster actuation for this correction is presented in Table 2.

The function of spacecraft ΔV for positioning or station change is also important. This would be performed by commanding a turn to orient the north–south thrusters in the line of the proposed change. Then, the north–south thrusters could be actuated together to perform the required impulsive maneuver (Fig. 12). For low-thrust maneuvers which are time-constrained, the thrusters will remain on for half the reposition longitude (Fig. 13). The

Table 1. Thruster actuation program for the generation of spacecraft torque

Option	Function	System	Thrusters required for torque and torque level					
			Axis 1		Axis 2		Axis 3	
			Thrusters required	Torque level, mN-m	Thrusters required	Torque level, mN-m	Thrusters required	Torque level, mN-m
I	1	N_2H_4	T1[a], T2	474.5	T3, T4	474.5	T5, T6	474.5
	2	N_2H_4	T1, T2	474.5	T3, T4	474.5	T5, T6	474.5
	3	N_2H_4	T1, T2	474.5	T3, T4	474.5	T5, T6	474.5
	4	N_2H_4	T1, T2	474.5	T3, T4	474.5	T5, T6	474.5
II	1	Inert gas	T1, T2	474.5	T3, T4	474.5	T5, T6	474.5
	2	Inert gas	T1, T2	474.5	T3, T4	474.5	T5, T6	474.5
	3	Ion	T1[b], T2[b]	3.39	T1[c], T2[c]	0.81	T3[c]	0.41
	4	Inert gas	T1, T2	474.5	T3, T4	474.5	T5, T6	474.5
III	1	Inert gas	T1, T2	474.5	T3, T4	474.5	T5, T6	474.5
	2	Inert gas	T1, T2	474.5	T3, T4	474.5	T5, T6	474.5
	3	PP[d]	T1, T2	6.1	T3, T4	5.15	T5, T6	4.1
	4	Inert gas	T1, T2	474.5	T3, T4	474.5	T5, T6	474.5
IV	1	N_2H_4	T1, T2	474.5	T3, T4	474.5	T5, T6	474.5
	2	N_2H_4	T1, T2	474.5	T3, T4	474.5	T5, T6	474.5
	3	N_2H_4	T1, T2	474.5	T3, T4	474.5	T5, T6	474.5
	4	N_2H_4	T1, T2	474.5	T3, T4	474.5	T5, T6	474.5
V	1	N_2H_4	T1, T2	474.5	T3, T4	474.5	T5, T6	474.5
	2	N_2H_4	T1, T2	474.5	T3, T4	474.5	T5, T6	474.5
	3	N_2H_4	T1, T2	474.5	T3, T4	474.5	T5, T6	474.5
	4	N_2H_4	T1, T2	474.5	T3, T4	474.5	T5, T6	474.5

[a]Designation of thruster number as presented in Figs. 7 and 8.

[b]Thruster turned on until maximum thrust (about 10 min) and turned off and allowed to decrease in thrust to off condition (about 10 min).

[c]Vectoring ±5 deg creates a spacecraft torque.

[d]Limit cycle operation without reaction wheels.

Table 2. Thruster actuation program for the generation of spacecraft translation

Option	Function	System	Thruster required for spacecraft translation
I	5	N_2H_4	T1 and T2 or T3 and T4
	6	N_2H_4	T5 and T6
	7	N_2H_4	T5 and T6
	8	N_2H_4	T1 and T2 or T3 and T4
II	5	Ion	T1 and T2
	6	Ion	T3
	7	Ion	T3
	8	Ion	T1 and T2
III	5	Pulsed plasma	T1 and T2 or T3 and T4
	6	Pulsed plasma	T5 and T6
	7	Pulsed plasma	T5 and T6
	8	Pulsed plasma	T1 and T2 or T3 and T4
IV	5	Pulsed plasma	T1 and T2 or T3 and T4
	6	Pulsed plasma	T5 and T6
	7	Pulsed plasma	T5 and T6
	8	Pulsed plasma	T1 and T2 or T3 and T4
V	5	Ion	T1 and T2
	6	Ion	T3
	7	Ion	T3
	8	Ion	T1 and T2

spacecraft is then turned 180 deg. For low-thrust maneuvers, the thrusters remain on for the remainder of the longitude correction. When the new station is reached, the thrusters are actuated for impulsive maneuvers. The spacecraft is then turned into its proper position. A summary of the proper thruster actuation to accomplish positioning or station change is presented in Table 2.

IV. Propulsion Requirements

Before attitude propulsion requirements can be estimated, all torques that tend to disturb the attitude of a spacecraft must be considered. These include the torques resulting from radiation forces on the spacecraft surfaces (Ref. 6), gravitational or gravity gradient torques (Ref. 7), aerodynamic torques resulting from the impingement of atmospheric gas molecules on spacecraft surfaces (Ref. 8), and the magnetic torques resulting from the interaction between magnetic properties of the spacecraft and the ambient magnetic field (Ref. 9). Aerodynamic torques were negligible except at the low altitude points during the first few days of spiral-out to synchronous orbit; hence they will not be discussed here. Magnetic torques are not discussed since they are small compared to radiation and gravity gradient torques.

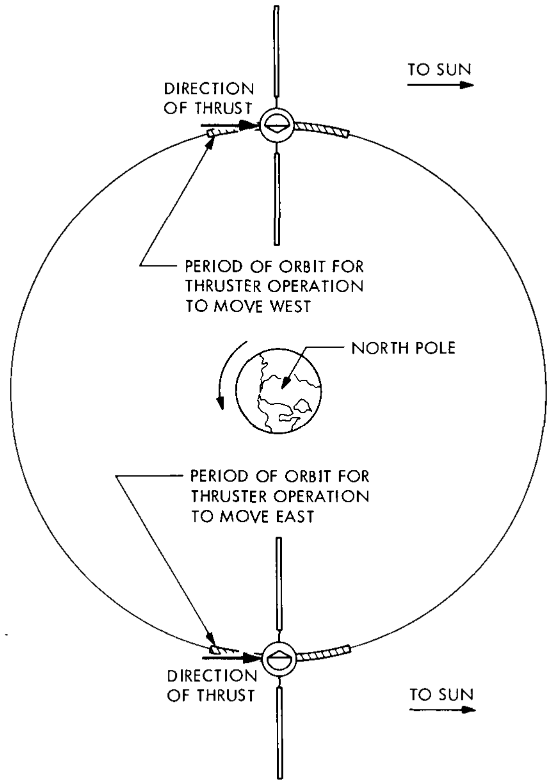

Fig. 10. Thrusting program for east–west stationkeeping

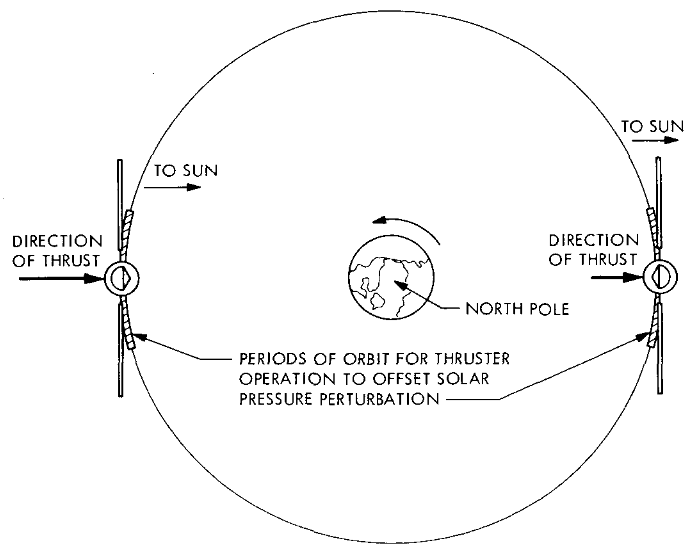

Fig. 11. Thrusting program for solar pressure orbit perturbation cancellation

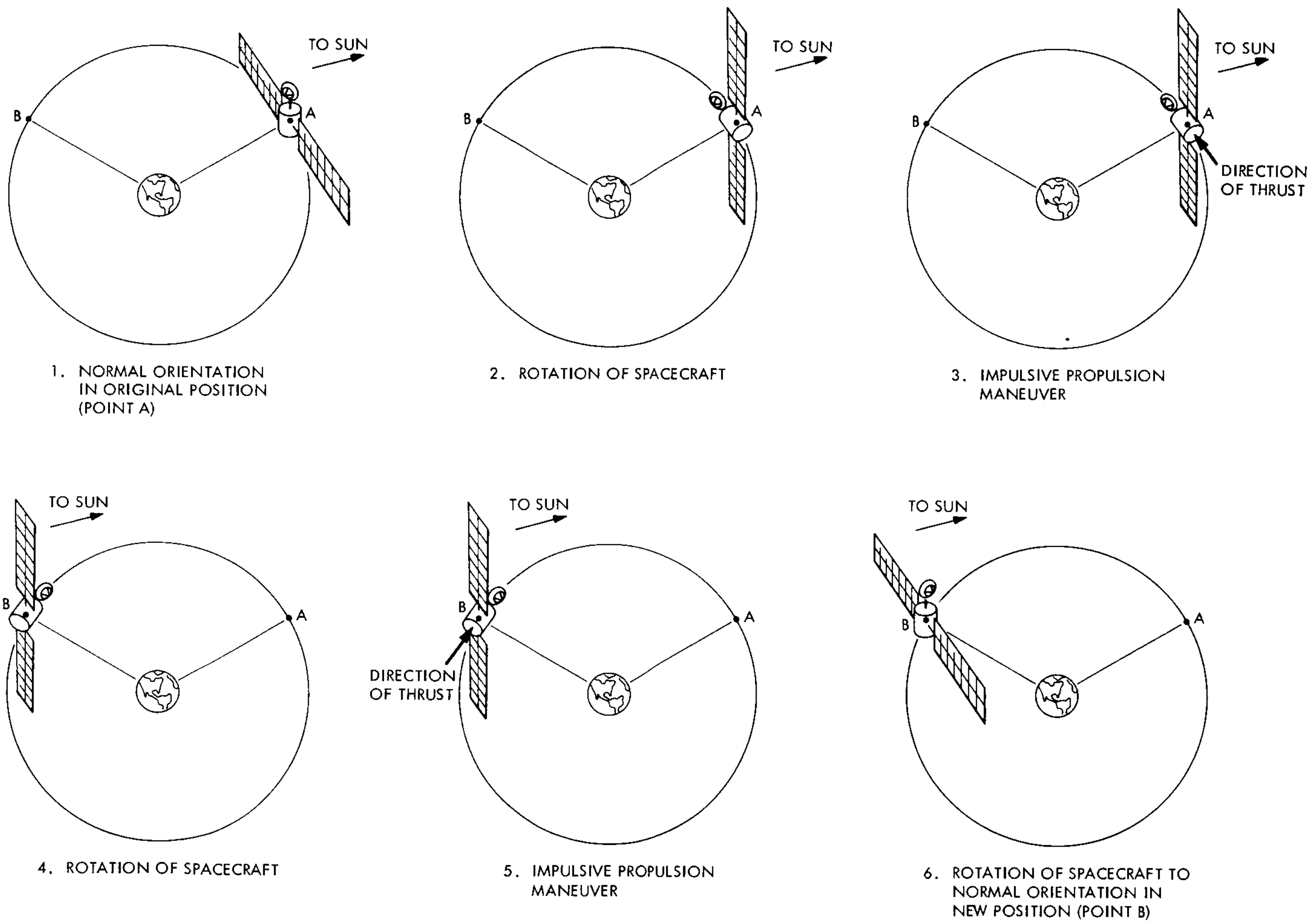

Fig. 12. Thrusting program for impulsive propulsion spacecraft reposition

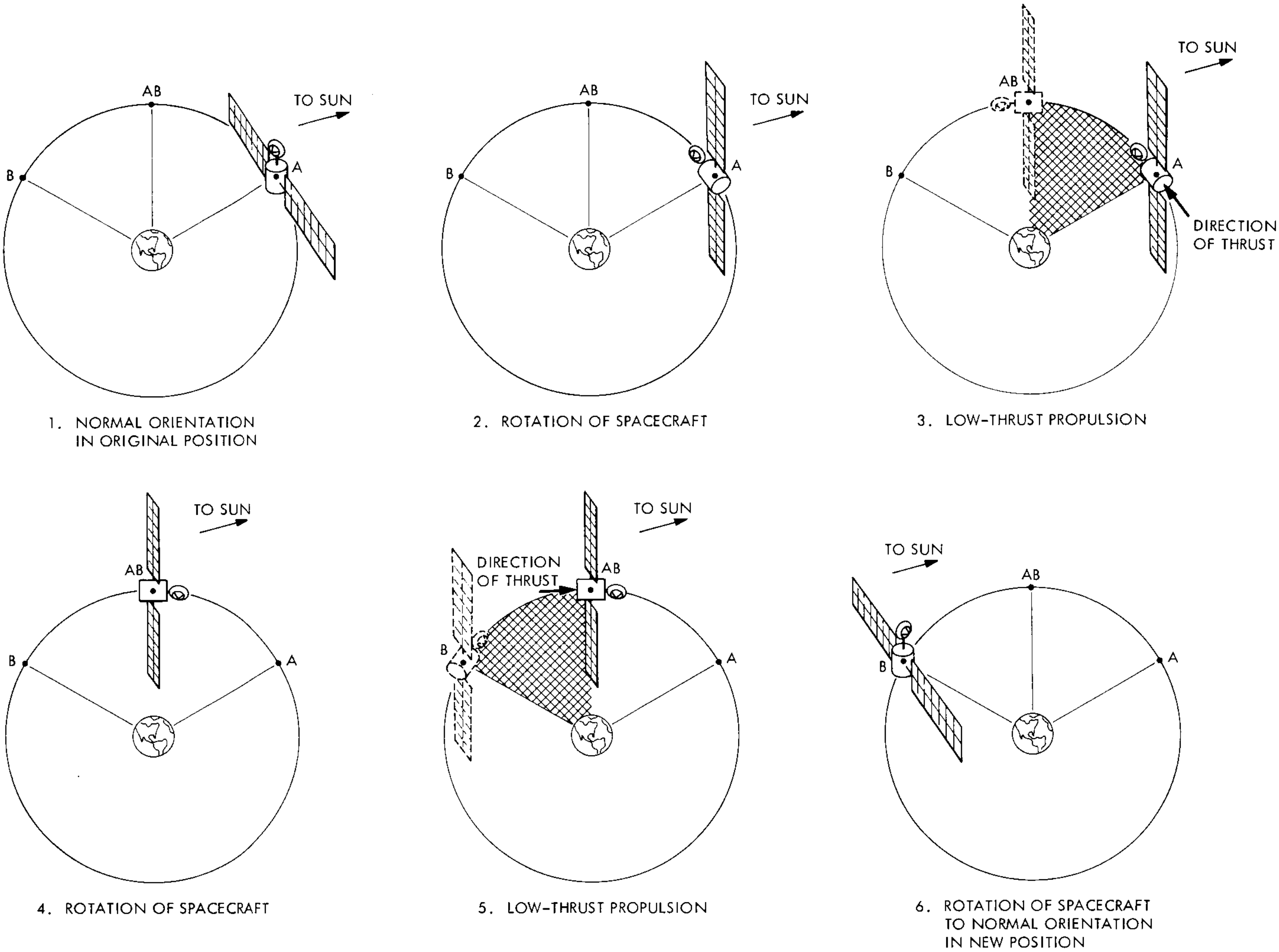

Fig. 13. Thrusting program for low-thrust electric propulsion spacecraft reposition

A. Radiation Torque

A general discussion of spacecraft radiation torques is given in Ref. 6. The center of radiation pressure (cp)/ center of gravity (cg) offset was presented earlier for each of the three primary axes. These values were calculated by estimating the projected area in each of the three axes and finding its center of pressure. With the knowledge of the spacecraft center of gravity, the cp/cg offset is known. See Ref. 6 for details as to the calculation of the center of pressure of simple geometric surfaces.

The next step in calculating radiation torques is to estimate the magnitude of the radiation force on the spacecraft surfaces. The general equation for solar radiation pressure is given by (see Figs. 14 and 15):

$$P_s = K_{I/C} \cos\theta \left[(1 - \rho_s) \cos\theta + \frac{2}{3} \rho_d \right] \quad (1)$$

which can be written

$$P_s = K_{I/C} \cos\theta \left[\left(\cos\theta + \frac{2}{3} \right) + \rho_{ds} (1 - A_{dr}) \left(\cos\theta - \frac{2}{3} \right) \right] \quad (2)$$

The torque is then given by

$$T = P_s A_p L \quad (3)$$

(See Nomenclature for symbol definitions.)

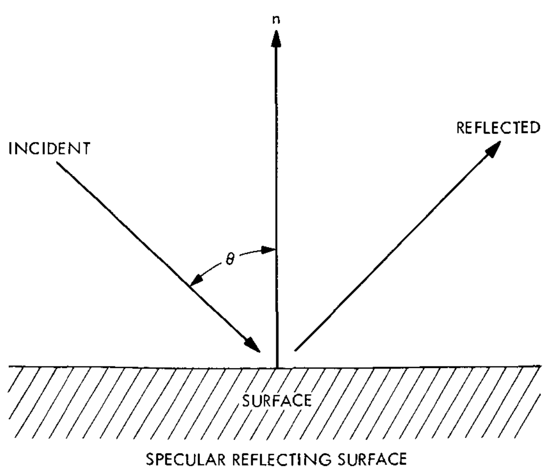

Fig. 14. Solar radiation pressure model for specular reflecting surfaces

For purposes of this report, values of 0.25 for the coefficient of reflectivity and 0.0 for the diffuse coefficient of reflectivity were assumed for solar arrays. The body and antenna were assigned values of 0.9 for the coefficient of reflectivity and 0.5 for the diffuse coefficient of reflectivity (Ref. 4). With these assumptions along with the surface area that was calculated from the spacecraft data of the previous section, curves of the solar radiation torques have been prepared and are portrayed in Figs. 16 and 17.

B. Gravity Gradient Torque

A general discussion of spacecraft gravity gradient torques is presented in Ref. 7. For preliminary design, estimation of the gravitational torques can be obtained by considering a satellite already in synchronous orbit. The satellite can be represented by six point masses separated by three massless rods as shown in Fig. 18. As the satellite is displaced in the pitch (axis 2) or roll (axis 3) plane, the gravitational torques are given by the following equations:

$$T_2 = \frac{3}{2} \omega_0^2 (I_3 - I_1) \sin 2\phi \quad (4)$$

$$T_3 = \frac{3}{2} \omega_0^2 (I_2 - I_1) \sin 2\delta \quad (5)$$

where

$$\omega_0 = \frac{gK}{a^3} \quad (6)$$

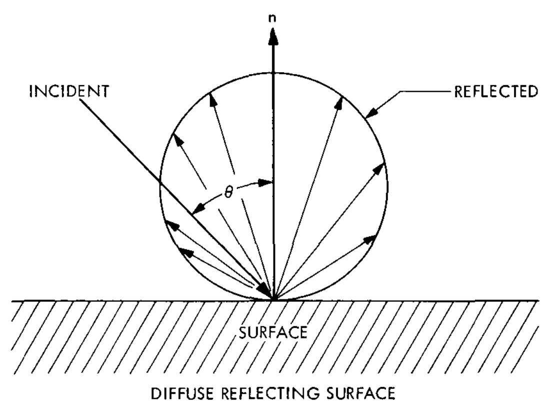

Fig. 15. Solar radiation pressure model for diffuse reflecting surfaces

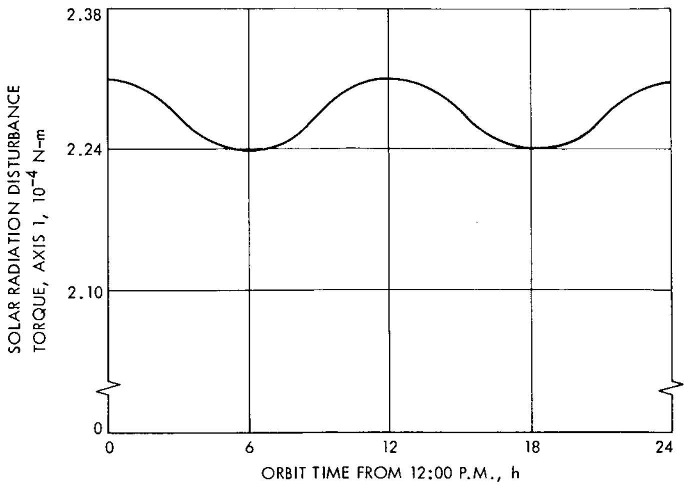

Fig. 16. Axis 1, solar radiation torque

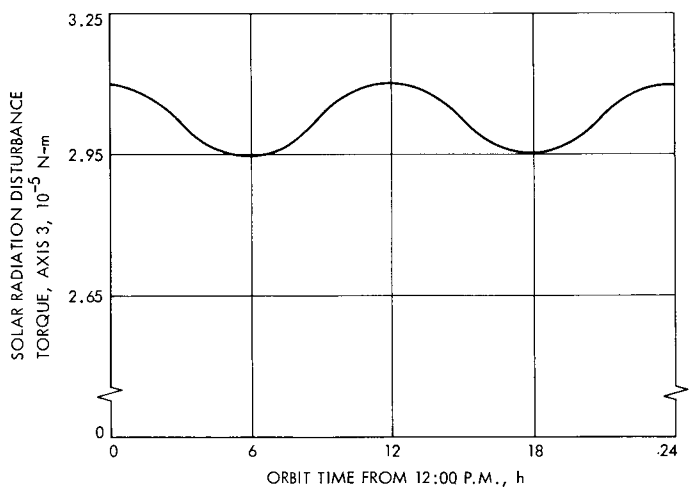

Fig. 17. Axis 3, solar radiation torque

Equation (6) is valid for circular orbits. Assuming a synchronous orbit and the spacecraft moments of inertia given in the previous section, the gravity gradient torques can be calculated. The spacecraft is stabilized in axis 2 and should not be displaced more than 0.1 deg. However, should an anomaly occur or the solar panels deflect greatly, a gravity gradient torque could occur about axis 2. A plot of the torque about axis 2 as a function of spacecraft displacement is given in Fig. 19. In axis 3 the spacecraft will undergo a sinusoidal value of gravity gradient torque (Fig. 20).

C. Momentum Storage Requirements

By integrating the solar pressure and gravity gradient torques, the momentum storage and propulsion requirements can be estimated. By taking the daily and yearly integral of torque requirements, the frequency of reaction wheel desaturation can be estimated along with the total propulsion requirements. These integrals are given in Table 3 (daily and yearly). For axis 2 a 30-min gravity gradient torque (spacecraft displaced 5 deg) is assumed to occur once during the day. Although this disturbance torque is not expected to occur, it is included. For reaction wheels with 2.9 m-N-s momentum storage capability in all three axes (wheels can have up to twice this value when unloaded from positive rotation, through zero, to negative rotation), the wheel in axis 1 must be unloaded four times per day, the axis 2 wheel can operate for more than a year without unloading, and the axis 3 wheel must be unloaded twice per day.

If a pulsed plasma system is used without reaction wheels the spacecraft will limit cycle. A study of the low-torque pulsed plasma system for the ATS-H spacecraft was conducted at JPL (Ref. 5). The conclusion of this study is that the disturbance torques that the spacecraft will experience are large enough so that the pulsed plasma system operates in a "one-sided" deadband, which means that the disturbance torques are sufficiently large that the spacecraft is never allowed to reach the second side of the attitude control deadband. This will render the limit cycle propulsion requirements for the pulsed plasma system equal to the integral of the disturbance torques (Table 3).

D. Spacecraft Tipoff Rate Reduction

This function is performed only once during the mission and occurs immediately after separation of the spacecraft from the launch vehicle. The general equation for tipoff rate reduction is given by:

$$t = \frac{I\Delta\dot{\theta}_{max}}{lF} \tag{7}$$

Table 3. Momentum storage requirements

Elapsed time	Axis 1, m-N-s	Axis 2, m-N-s	Axis 3, m-N-s
24-h day	19.6	0.4	5.2
1 yr	7,145	122	1870

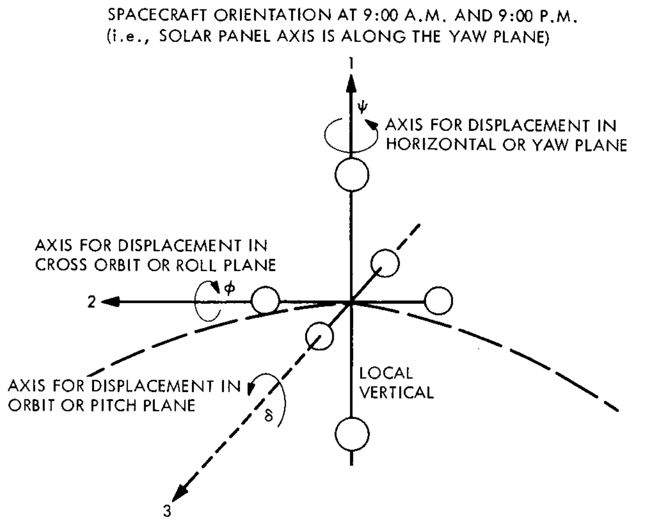

Fig. 18. Angular displacement model for gravity gradient torque

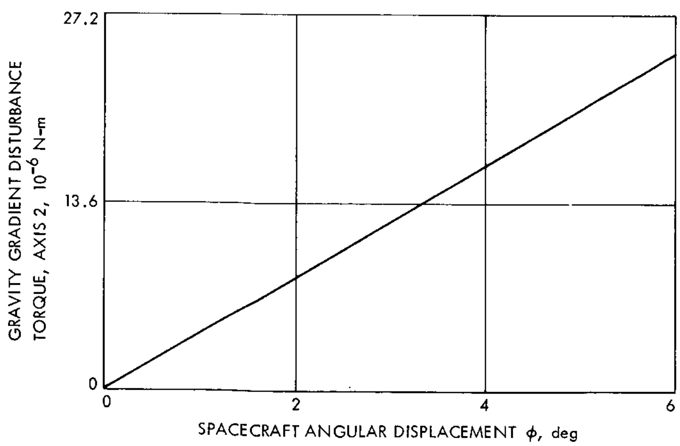

Fig. 19. Axis 2, gravity gradient torque as a function of spacecraft displacement

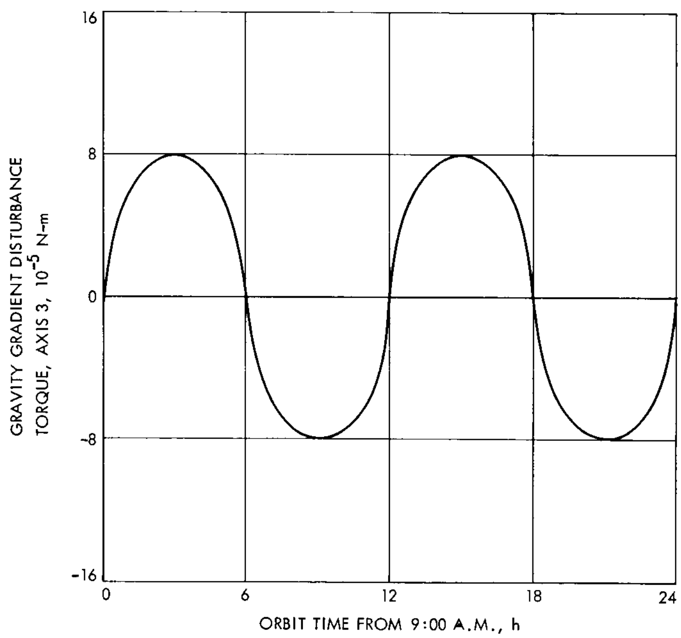

Fig. 20. Axis 3, gravity gradient torque

For a tipoff rate of 1 deg/s per axis, along with spacecraft moments of inertia and thruster torque levels given in the previous section, the tipoff rate reduction time can be calculated from Eq. (7). This time ranges from 45 min to 10 h for the torque levels of the ion and pulsed plasma systems. These times are too long, since the spacecraft must finish this maneuver before deployment of the solar panels can be accomplished. Without the solar panels deployed, the electric thrusters will rapidly deplete battery storage capability. It is for this reason, along with the times required to do acquisitions and commanded maneuvers, that the ion and pulsed plasma systems are paired with inert gas or hydrazine high torque systems. When higher electric propulsion torques are used, it becomes possible for electric propulsion systems to perform all mission functions (Ref. 10). The impulse required for this maneuver is given by

$$\text{Impulse} = tF = \frac{I\Delta\dot{\theta}_{\max}}{l} \tag{8}$$

For the ATS-H mission, the tipoff rate reduction maneuver propulsion requirements are small compared to the other functional requirements.

E. Acquisition

The spacecraft is accelerated to an angular rate of about 0.2 deg/s about axes 1 and 3 (or possibly 2) searching for the sun sensor nulls. In fact, pulsed plasma and ion torque levels of at least 10 times those given in the previous section would be required for this maneuver (0.2 deg/s). Thus only inert gas or hydrazine torque levels will be used for this function. Two equations for calculating acquisition propulsion requirements are:

$$\text{Impulse} = 2\,\frac{I\Delta\dot{\theta}_{\max}}{l} \tag{9}$$

$$\theta_s = \frac{\dot{\theta}^2{}_{\max} I}{2lF} \tag{10}$$

Equation (9) gives the impulse required to initiate and stop a search for a reference. Each acquisition requires that two axes must search for the sun. This comes to a total of 245 to 467 N-s per acquisition, which is small compared to other functional requirements. Equation (10) determines how many degrees the spacecraft rotates during the stopping of a search. This is important since the spacecraft should stop within the field of view of the sensors. For coarse sun sensors this is up to 120 deg, but for fine sensors it can be as low as 15 deg. For the torque levels of the hydrazine and inert gas systems the values of θ_s range from 0.5 to 10 deg. These stopping angles are adequate for the sensors on the ATS-H spacecraft.

F. Commanded or Unusual Incident Maneuvers

These maneuvers can be estimated by assuming that each is similar to an acquisition type of maneuver for a spacecraft angular acceleration to 0.2 deg/s rotational velocity (complete spacecraft rotation of 180 deg in 15 min) and deceleration to zero at the new point. Thus Eq. (9) can be used to estimate the propulsion requirement. This results in about 13.3 N-s per commanded turn about axis 1. The spacecraft can be pointed in any required direction when rotating about any two axes (236 N-s). The total number of these types of maneuvers is small and is only a small portion of the spacecraft propulsion requirements.

G. North–South and East–West Stationkeeping

The perturbation of a synchronous satellite orbit has been studied in detail and reported in several documents (Refs. 11, 12). The stationkeeping propulsion requirements of a synchronous satellite can be of three general orders of magnitude. The first is to correct for east–west orbit perturbations only and allow the spacecraft to drift at a rate of about 1 deg per year in the north–south direction. The second allows for north–south corrections of nearly 1 deg per year. This keeps the spacecraft in an area of approximately 24 km about a certain point, which is equivalent to about a 0.04 deg pointing error. The third is to include corrections for diurnal or short-term perturbations such as those caused by earth–moon effects. This type of correction will keep the spacecraft in a circular area of about 15.2 to 30.5 m and be equivalent to a 5×10^{-5} deg pointing error. It becomes apparent that the third type of stationkeeping would be required only for precise navigational satellites or satellite-to-satellite type networks.

The long-term or secular east–west drift of a satellite in synchronous orbit is caused by the asphericity of the earth. The velocity increment needed to remove this perturbation will vary as the longitudinal distance from the satellite to the nearest "gravity valley," where no east-west drift occurs. The two primary "gravity valleys" of the earth occur over the Indian Ocean (73°E) and over the Pacific Ocean (253°E). A plot of the east–west stationkeeping requirements as a function of spacecraft longitude is given in Fig. 21. A good rule of thumb is to assume a maximum of 2.1 m/s per year.

A velocity increment is required to correct for long-term drift of the satellite in the north–south direction due to slow tilting of the orbital plane away from the equatorial plane. This slow tilting is due to the forces of the sun and the moon which are not located in the equatorial plane of the earth. The orbit perturbation is a slow varying function of time as shown in Fig. 22 (Ref. 12). As an approximation, one can assume 53.3 m/s per year for north–south stationkeeping executed near the nodal points of an orbit as shown in Fig. 9. If thrusting times are from 1½ h before the nodal point to 1½ h after the nodal point, the cosine losses can be ignored (less than 5% of the total north–south stationkeeping requirement).

The diurnal in-track velocity increment requirements are not discussed here since such precise stationkeeping is not required for the ATS-H spacecraft. This correction is very large and usually requires at least 106.7 m/s per year. To convert these velocity increments into propellant mass, the Tsiolkovskii equation can be used:

$$\Delta V = C \ln \frac{M_0}{M_f} = C \ln \frac{1}{1 - \dfrac{M_p}{M_0}} \tag{11}$$

where

$$C = I_{sp} g_c$$

For a small auxiliary propulsion system ($M_p/M_0 << 1$) then, Eq. (11) can be simplified to

$$M_p = \frac{M_0 \, \Delta V}{I_{sp} g_c} \tag{12}$$

Using the appropriate equation (11 or 12) to calculate the value of M_p, we obtain

$$\text{Total impulse} = M_p I_{sp} g_c \tag{13}$$

H. Solar Pressure Orbit Perturbations

For most satellites this orbit perturbation can be ignored. However, when large rollout solar arrays are used, this orbit correction can become significant. Essentially this correction is equal to one-half the integral of the solar radiation force on the solar array. The solar radiation force is given by

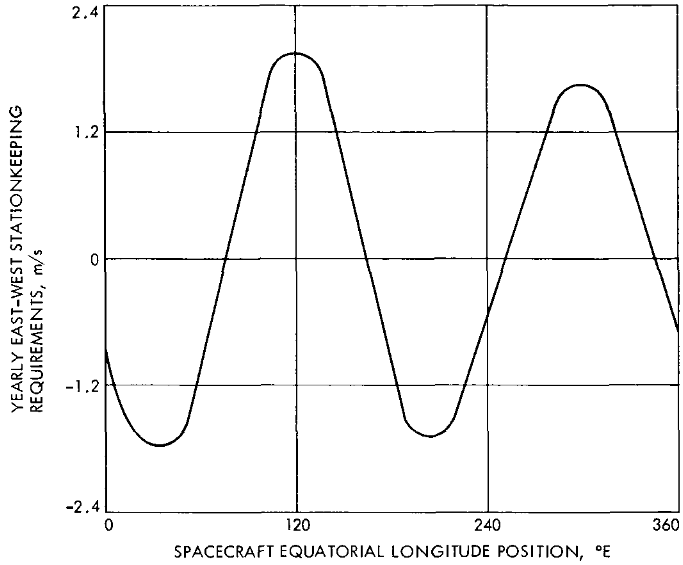

Fig. 21. East–west stationkeeping propulsion requirement

$$F_{\text{solar}} = (A_{sp}) \int_0^t P_s(t)\, dt \tag{14}$$

where $P_s\ (t)$ is really Eq. (1) with θ replaced by t. At $\theta = 0$, the orbit begins at $t = 0$, and at $\theta = 360$ deg, the orbit is complete at $t = 24$ h.

The factor of one-half comes from a $\sin^2 \theta$ term. As the satellite moves about its orbit, only the portion of the solar force that is normal to the spacecraft orbit velocity will perturbate the orbit, while that which is in the direction of the velocity will cancel itself out during one complete orbit. Using the solar pressure values given previously, a solar pressure perturbation correction of 16,013 N-s per year is required. This is equivalent to about 22.9 m/s in velocity change. These corrections will be performed at the points depicted in Fig. 11.

I. Spacecraft ΔV for Positioning or Station Change

This function is strongly dependent on the time allowed for positioning or station change and the number of times repositioning will occur (Refs. 11, 12). For purposes of this study the satellite is assumed to be placed over the United States and maintained there for the duration of the mission. With a high-thrust chemical system such as hydrazine, these functions can be performed with about half the amount of spacecraft velocity change of a low-thrust electric thruster which is required to be on for the entire reposition time. The interrelationship of reposition time, repositioning angle, and thrust level is presented in Fig. 23. This figure is for low-thrust propulsion systems such as the ion or pulsed plasma systems that are thrusted continuously during the maneuver. With a hydrazine propulsion system which will operate impulsively, the velocity increment can be reduced by half. A requirement of 15.2 m/s for removal of launch errors (Ref. 11) is assumed for this mission and no total impulse for spacecraft reposition has been included. The station change function can require considerably more propellant allocation, especially if repositioning is desired.

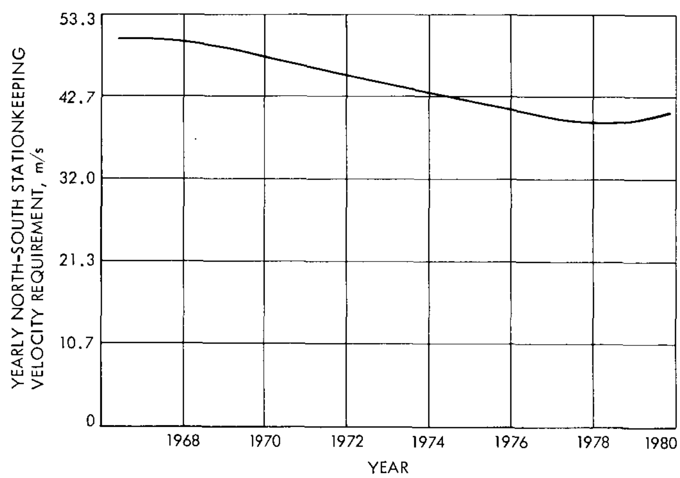

Fig. 22. North–south stationkeeping propulsion requirements

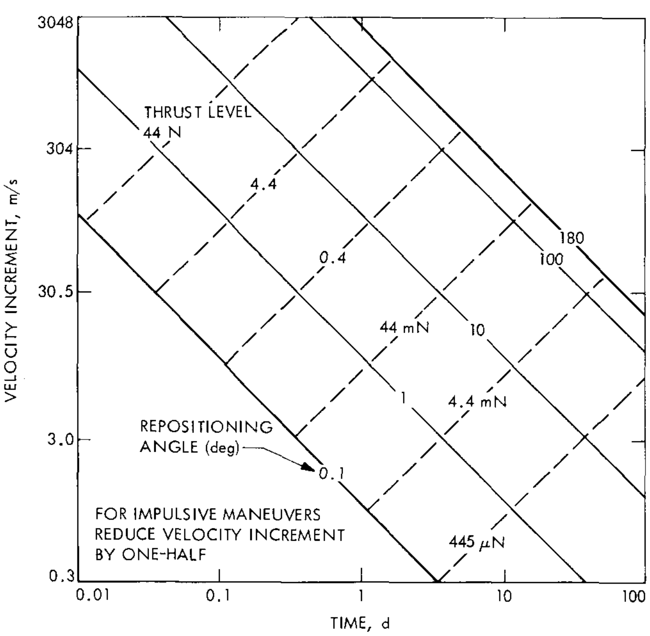

Fig. 23. Low-thrust spacecraft reposition propulsion requirements

J. Summary of Propulsion Requirements

The propulsion requirements are summarized in Table 4. The mass of each system's option then is calculated assuming these requirements for 5 years. The velocity increments of functions 5, 6, 7, and 8 can be converted to propellant mass with Eq. (11).

V. Candidate Systems and Characteristics

As discussed previously, there are five candidate system options. The propulsion types are inert gas, catalytic hydrazine, mercury ion bombardment (5 cm), and pulsed plasma (high energy). These systems have been discussed in detail in Refs. 1 and 2. Some of the system data has been modified as a result of recent testing.

A. System Performance and Power

Performance and power requirements of the candidate systems are presented in Table 5. Performance data for the 5-cm ion bombardment thruster is from recent test results at Hughes Research Laboratory (HRL).

B. System Mass

Two levels of redundancy were used for this study. The first was a single system configuration with the minimum number of thruster assemblies. This means that six thrusters were used for the inert gas, pulsed plasma, and catalytic hydrazine systems, while three thrusters were required for the ion thruster system. The more reliable double system options incorporated twice the minimum number of thrusters, with two thrusters per required location. Hardware mass was estimated from data provided in Refs. 1 and 2. Two important mass relationships for the pulsed plasma system are a capacitor mass of 0.22 kg/J and power conditioning mass of 500 g plus 11 g per watt of power. Mercury bombardment thruster mass was taken from present HRL data. The hydrazine and inert gas systems employed dual series solenoid valves in both levels of redundancy. Thruster hardware mass is presented in Table 6. The thrust level of each device, the power required and its mass penalty with solar power specific mass of 13.6 W/kg, propellant and tankage mass, and the total mass for each option are included in this table. The torque levels, moment arms,

Table 4. Propulsion requirements

Function	Functional requirement: Thruster axis 1	Thruster axis 2	Thruster axis 3	Velocity increments
1. Spacecraft tipoff rate reduction, N-s	48.48	64.94	64.94	
2. Five acquisitions, N-s	13.34	235.74	229.07	
3. Momentum storage requirements, N-m-s	7,144.8	122.02	1,870.94	
4. Five commanded turns, N-s	13.34	–	229.07	
5. North–south stationkeeping, m/s				53.34
6. East–west stationkeeping, m/s				2.13
7. Solar pressure orbit perturbations, m/s				22.86
8. Spacecraft positioning or station change, m/s				15.24

Table 5. Performance and power data

Propulsion system type	Specific impulse, N-s/kg	Thruster power thrust, W/mN	Power conditioning efficiency, %
Inert gas	706	–	–
Hydrazine catalyst	2,140	–	–
Ion bombardment	29,420	32.0	85.0
Pulsed plasma	12,200	35.0	85.0

and propulsion requirements presented in the previous sections were combined to calculate the required propellant mass. Pulsed plasma options that operate in a limit cycle mode require additional propellant in each thruster because of the uncertainty as to which thruster would be required to counter spacecraft disturbance torques. Also, to achieve complete system redundancy, the pulsed plasma propellant mass has to be doubled when twice the number of thrusters is used. This is because its solid propellant is not usable if a thruster should fail. For the pulsed plasma option III (propulsion system operates in a limit cycle mode), the mass of the reaction wheels and their power requirements are subtracted from the total system mass. The equivalent mass reduction is 14.1 kg and has been factored into Table 6.

Thrust levels of the system options are also given in Table 6. Inert gas and hydrazine systems were given thrust levels of 0.4 N in order to provide a sufficient torque level for commanded maneuvers and acquisitions. The thrust levels of the ion systems were calculated by dividing the required total impulse of each thruster by 10,000 hours, which is the expected life of each thruster. The result is that for all ion thrusters to have sufficient total impulse capability in system option II, a thrust level of 4.5 mN is required, and in system option V a thrust level of 3.3 mN is required. The impulse bit per pulse of the pulsed plasma system was calculated by dividing the required total impulse of each thruster by 10^7 pulses. This results in an impulse bit of 6.67×10^{-3} N-s/pulse for option III and an impulse bit of 4.48×10^{-3} N-s/pulse for option IV. These values will size the thruster and capacitor. The power required for this mission is "cheap" since rollout arrays are used. Therefore, the thrust level or power consumption of these devices can be high without a severe mass penalty. At one pulse per second, the thrust levels for system options III and IV become 4.67 mN and 4.45 mN, respectively.

C. System Reliability

Reliability values for the inert gas and hydrazine systems were taken directly from Table C-4, Appendix C, of Ref. 1. The system redundancy configurations used in this report are referred to as single and double redundancy. These configurations were referred to in Ref. 1 as single-system single- or dual-series solenoid (corresponding to single redundancy herein) and single-system 12-thrust chambers with dual-series solenoid (corresponding to double redundancy herein). The inert gas system was assumed to require 1000 actuations (tipoff rate reduction, acquisitions, and commanded maneuvers), while the hydrazine system was assumed to require 10,000 actuation series for five years of attitude propulsion. Propulsion system reliability values are tabulated in Table 7. The reliability numbers for ion and pulsed plasma systems presented in Table 7 have not been reported previously.

Table 6. System option mass data

System	Option	Redundancy level	Thrust level, mN	Hardware mass, kg	Power required, W	Power penalty, kg	Propellant and tankage mass, kg	Option total mass. kg
I	Hydrazine	Single	444.8	2.18	–	–	177.17	179.35
I	Hydrazine	Double	444.8	4.35	–	–	177.17	181.53
II	Ion		4.448	24.22	330	4.99	5.22	
	and	Single			(Two at a time)			41.87
	inert gas		444.8	2.90	–	–	4.54	
II	Ion		4.448	48.44	330	4.99	5.22	
	and	Double			(Two at a time)			67.99
	inert gas		444.8	4.81	–	–	4.54	
III	Pulsed plasma		6.672	91.85	825	12.47	30.39	
	and	Single			(Three at a time)			128.09[a]
	inert gas		444.8	2.90	–	–	4.54	
III	Pulsed plasma		6.672	183.70	825	12.47	60.55	
	and	Double			(Three at a time)			252.01[a]
	inert gas		444.8	4.81	–	–	4.54	
IV	Pulsed plasma		4.448	64.77	365	5.53	23.59	
	and	Single			(Two at a time)			121.61
	hydrazine		444.8	2.18	–	–	25.54	
IV	Pulsed plasma		4.448	129.55	365	5.53	47.17	
	and	Double			(Two at a time)			121.65
	hydrazine		444.8	4.35	–	–	25.54	
V	Ion		3.336	24.22	250	3.76	3.36	
	and	Single			(Two at a time)			59.06
	hydrazine		444.8	2.18	–	–	25.54	
V	Ion		3.336	48.44	250	3.76	3.36	
	and	Double			(Two at a time)			85.46
	hydrazine		444.8	4.35	–	–	25.54	

[a]Reduced 14.1 kg for reaction wheel removal.

Table 7. System reliability data

Propulsion system type	Reliability type	Reliability of thruster and power conditioner system (single redundancy)
Monopropellant hydrazine	–	0.90
Inert gas	–	0.89
Ion	HRL	0.78
Ion	TRW	0.69
Ion	Life test	0.31
Pulsed plasma	High-reliability capacitor	0.79
Pulsed plasma	Life test	0.55

For the ion thruster systems, three sources of reliability were used. The first is presented in Ref. 13. This unpublished report presents a detailed analysis of ion propulsion system reliability. The power conditioning circuits are broken into component types and individual component failure rates are assigned. Included in the power conditioning system are a control logic module and a vectoring supply module (to provide beam vectoring). The thruster is broken into its components, weld lengths, and braze joints. In order to account for cycling of certain components (e.g., heaters), a cyclic failure rate has been added to the final failure rate by the author. It has been argued that the constant failure rate of an ion thruster is valid for only 7000–8000 h, at which time the thruster failure rate will increase rapidly because of wearout. For purposes of this study, however, a 10,000-h life and a constant failure rate were assumed. The thruster was assumed to be cycled a maximum of 1000 times. The true cyclic failure rate of an ion thruster is really unknown, since most "life" tests which have been performed on ion thrusters to date have been steady-state, with only a few thruster on-off cycles (usually less than 10). The resulting thruster and power conditioning reliability for 10,000 h of operation is 0.92.

Ion thruster reliability is also investigated in Ref. 14. This report attempts to compare the manufacturing, electrical, and thermal similarities between ion thrusters and high-level traveling wave tubes (TWTs), it being assumed that the latter have a failure rate of $\lambda = 3025 \times 10^{-9}$ failures/h. From this study a failure rate of $\lambda = 5900 \times 10^{-9}$ failures/h is estimated for an ion thruster. This value was again modified for cyclic failure rates. The resulting thruster and power conditioning reliability for this mission is 0.89.

A third ion thruster reliability was calculated by taking test data from long-term ion thruster life tests and calculating a thruster failure rate. Most of the life tests conducted to date have been referred to by many as "development tests," where thruster operation was terminated at the first sign of malfunction. Others have criticized the results of life tests as being invalid when tests are performed in vacuum facilities instead of space. Very few long-life ion thruster tests have been conducted where the thruster is carefully watched and kept in a true space environment. This is primarily due to the extremely high cost of such tests. It is hoped that as longer and longer life tests of ion thrusters are performed in "spacelike" environments, ion thruster failure rates will be reduced. It is assumed that a system reliability based on present life test data is a lower limit to ion thruster reliability (for steady-state thruster operation). The resulting thruster and power conditioning (life test) reliability is 0.68.

The three thruster reliabilities listed above were all calculated by the author and include additional factors for thruster cycling. The absolute magnitudes of these reliabilities vary greatly; the sensitivity of the final results to these values is discussed in a subsequent section herein.

For pulsed plasma thruster systems, three additional sources of component reliabilities have been used—JPL electronic component failure rates,[2] Capacitor Specialists Incorporated,[3] and Fairchild Hiller.[4] The circuit diagram of the LES-6 pulsed plasma power conditioning system was compared to the HRL ion thruster power conditioning circuit diagram in order to establish a relative value of pulsed plasma power conditioning reliability. The circuit diagram of a pulsed plasma thruster which includes redundant spark igniter capacitor circuits and a high-energy storage capacitor was used to calculate the pulsed plasma thruster reliability. Capacitor data was averaged from laboratory test data. The resulting pulsed plasma thruster reliability for a life of 10^7 pulses is 0.96 (with high-reliability capacitor). A second pulsed plasma reliability was calculated by taking test data from long-term pulsed plasma system tests and calculating a failure rate. Very little long-life test data is available. It is hoped that as more experience with this system is acquired, failure rates will be reduced. It is assumed that a pulsed plasma thruster reliability based on present life test data is a lower limit to system reliability. The resulting thruster and power conditioning reliability (life test) is 0.9.

The individual system reliabilities are combined to form the five system options. The total auxiliary propulsion system reliability is then given in Table 8. The reliability of option III systems has been increased by a factor to account for the removal of reaction wheels from the spacecraft. Reaction wheel failure rates were based on JPL data and on failure rates for AC motors (Ref. 15).

D. System Cost

The costs of the inert gas systems were taken directly from Appendix D of Ref. 1. The cost of the hydrazine

[2]Industry briefing ("Thermoelectric Outer Planets Spacecraft"), Jet Propulsion Laboratory, Pasadena, Calif., Sept. 28, 1971.

[3]Personal communication from Bruce Hayworth, Capacitor Specialists, Inc., San Diego, Aug. 1971.

[4]Personal communication from W. Guman, Fairchild Hiller Corp., Farmingdale, N.Y., Jan. 1972.

Table 8. System option reliability data

Option	Redundancy level	Reliability type	Reliability of system option
I	Single	-	0.90
I	Double	-	0.99
II	Single	HRL	0.69
II	Single	TRW	0.61
II	Single	Life Test	0.27
II	Double	HRL	0.96
II	Double	TRW	0.95
II	Double	Life Test	0.71
III	Single	High-reliability capacitor	0.71[a]
III	Single	Life test	0.49[a]
III	Double	High-reliability capacitor	0.99[a]
III	Double	Life test	0.95[a]
IV	Single	High-reliability capacitor	0.71
IV	Single	Life test	0.50
IV	Double	High-reliability capacitor	0.98
IV	Double	Life test	0.94
V	Single	HRL	0.70
V	Single	TRW	0.62
V	Single	Life test	0.28
V	Double	HRL	0.97
V	Double	TRW	0.95
V	Double	Life test	0.71

[a]Increased to account for reaction wheel removal.

Table 9. System option cost data

Option	Redundancy level	Number of propulsion system	Total systems cost, $ millions
I	Single	1	1.0
I	Double	1	1.2
II	Single	2	2.0
II	Double	2	2.35
III	Single	2	0.95[a]
III	Double	2	1.30[a]
IV	Single	2	1.8
IV	Double	2	2.3
V	Single	2	2.6
V	Double	2	2.9

[a]Reduced cost for removal of reaction wheels.

propulsion system is based on current costs of the catalytic monopropellant hydrazine systems for the ATS-F and -G and Canadian Technology Satellite programs. The ion bombardment thruster costs were obtained from discussions with HRL (Ref. 3). Costs for the pulsed plasma thruster systems were based on discussions with Fairchild Hiller and the SMS satellite program.[5] Costs presented in Table 9 are based on the following basic constraints:

(1) 1972 dollars.

(2) Engineering test model (at least one full-up system).

(3) Vibration and thermal systems (can be mock-ups).

(4) Type approval and proof test systems (can use same hardware with refurbishment).

(5) Flight system.

(6) Spare components.

System costs include ground support equipment and testing to be performed by contractors. Systems were assumed to have been qualified prior to program start.

VI. Comparisons and Sensitivity Analysis

System comparisons will be performed using the cost effectiveness techniques described in Section II of Ref. 1. These comparisons serve as additional examples of the techniques previously discussed. In addition, the sensitivity of the final results to mission assumptions and candidate system characteristics will be discussed.

A. Mission Assumptions and Cost Effectiveness Coefficients

Assignment of mission worth, probability of success, and cost have been discussed. The next step in the tradeoff of candidate thruster systems is the calculation of mass, reliability, and cost "influence coefficients." The method of calculation of these coefficients is discussed in Section II of Ref. 1. These calculations are displayed as follows:

$$CE_{\text{baseline}} = \frac{\sum_i P_i W_i}{\sum_i C_i} \tag{15}$$

[5]Personal communication from R. Callens, Goddard Space Flight Center, Greenbelt, Md., April 1972.

where

P_i = probability of success (Fig. 2)

W_i = mission worth (Fig. 1)

$\sum_i C_i$ = total mission cost of $120 million

$$CE_{\text{baseline}} = \frac{(96)(0.545) + (92)(0.468) + (88)(0.402) + (84)(0.345) + (80)(0.207)}{\$120} = 1.529 \; \frac{\text{units}}{\$ \text{ million}}$$

The cost effectiveness of the mission with the addition of 136.1 kg of mass to system redundancy becomes

$$CE = \frac{(96)(0.601) + (92)(0.568) + (88)(0.537) + (84)(0.507) + (80)(0.480)}{\$120} = 1.985 \; \frac{\text{units}}{\$ \text{ million}}$$

Therefore the change in cost effectiveness per kg for the addition of 0 to 136.1 kg redundancy mass is

$$\frac{\Delta CE}{\Delta \text{mass}} = \frac{1.985 - 1.529}{136.1} = 3.35 \times 10^{-3} \; \frac{\left(\frac{\text{units}}{\$ \text{ million}}\right)}{\text{kg}}$$

The cost effectiveness of the mission with the addition of 226.8 kg of mass to system redundancy becomes

$$CE = \frac{(96)(0.620) + (92)(0.600) + (88)(0.592) + (84)(0.578) + (80)(0.565)}{\$120} = 2.171 \; \frac{\text{units}}{\$ \text{ million}}$$

Therefore the change in cost effectiveness per kg for the addition of 136.1 to 226.8 kg redundancy mass is

$$\frac{\Delta CE}{\Delta \text{mass}} = \frac{2.171 - 1.985}{90.7} = 2.05 \times 10^{-3} \; \frac{\left(\frac{\text{units}}{\$ \text{ million}}\right)}{\text{kg}}$$

The cost effectiveness of the mission with an increase in subsystem reliability of 0.01 (0.90 to 0.91) is

$$CE = \frac{\frac{0.91}{0.90}\left[(96)(0.545) + (92)(0.468) + (88)(0.402) + (84)(0.345) + (80)(0.297)\right]}{\$120} = 1.546 \; \frac{\text{units}}{\$ \text{ million}}$$

Therefore the change in cost effectiveness for reliability increase is

$$\frac{\Delta CE}{\Delta \text{reliability}} = \frac{1.546 - 1.529}{0.01} = 1.70 \; \frac{\left(\frac{\text{units}}{\$ \text{ million}}\right)}{\text{increase in reliability}}$$

The cost effectiveness of the mission with an increase in total mission cost of $1 million is

$$CE = \frac{(96)(0.545) + (92)(0.468) + (88)(0.402) + (84)(0.345) + (80)(0.297)}{\$121} = 1.516 \; \frac{\text{units}}{\$ \text{ million}}$$

Therefore the change in cost effectiveness per million dollar increase in total mission cost is

$$\frac{\Delta CE}{\Delta \text{cost}} = 1.516 - 1.529 = -1.26 \times 10^{-2} \; \frac{\left(\frac{\text{units}}{\$ \text{ million}}\right)}{\$ \text{ million}}$$

The effect of modified mission worth, probability of success, and program cost is shown in Table 10. Data from Figs. 1–5 has been used along with modified values of mission cost.

B. Comparisons of Candidate Systems

System I with single redundancy is assigned as the baseline system from which all comparisons are referenced. The difference in cost effectiveness between the baseline system and any other system is given by

$$\Delta CE = \frac{\Delta CE}{\Delta \text{mass}} \Big| \Delta \text{mass} + \frac{\Delta CE}{\Delta \text{cost}} \Big| \Delta \text{cost} + \frac{\Delta CE}{\Delta \text{reliability}} \Big| \Delta \text{reliability} \tag{16}$$

where Δmass, Δcost, and Δreliability are the differences in the baseline and comparative system mass, cost, and reliability (deltas). These deltas are presented in Table 11, which is based on data from the previous section. The terms $\Delta CE/\Delta$mass, $\Delta CE/\Delta$cost, and ΔCE/reliability are called "influence coefficients" and are given in Table 10.

The difference in cost effectiveness between the baseline and other system options can be calculated from Eq. (16), using the "deltas" given in Table 11 for the candidate system options and the "influence coefficients" given in Table 10. The baseline influence coefficients have been used for preliminary system comparisons; the other "influence coefficients" presented in Table 10 will be used later to examine the sensitivity of the results to the mission assumptions. In order to gain a perspective as to the magnitude of cost effectiveness differences, a dollar value can be assigned to this difference. Although it is difficult to assign a dollar magnitude to the product of worth times probability of success for any given mission, as a minimum, a dollar value equal to satellite cost could be assumed. This is to say that the returns

Table 10. Influence coefficients for various mission assumptions

Parameter	Baseline data	Increased mission worth	Decreased mission worth	Modified probability of success	Decreased mission cost	Increased mission cost
Probability of success from figure	2	2	2	3	2	2
Mission worth from figure	1	1	1	1	1	1
Total mission cost, \$ million	120	120	120	120	100	140
Baseline cost effectiveness, $\left(\frac{\text{units}}{\$ \text{ million}}\right)$	1.53	1.71	1.34	1.25	1.83	1.31
$\frac{\Delta CE}{\Delta \text{mass}^a}, \left(\frac{\frac{\text{units}}{\$ \text{ million}}}{\text{kg}}\right)$	6.89×10^{-4}	8.03×10^{-4}	5.81×10^{-4}	1.35×10^{-3}	8.30×10^{-4}	5.94×10^{-4}
$\frac{\Delta CE}{\Delta \text{mass}^b}, \left(\frac{\frac{\text{units}}{\$ \text{ million}}}{\text{kg}}\right)$	4.23×10^{-4}	4.94×10^{-4}	3.47×10^{-4}	3.01×10^{-4}	5.08×10^{-4}	3.62×10^{-4}
$\frac{\Delta CE}{\Delta \text{reliability}}, \left(\frac{\frac{\text{units}}{\$ \text{ million}}}{\text{increase in reliability}}\right)$	1.70	1.90	1.49	1.39	2.04	1.45
$\frac{\Delta CE}{\Delta \text{cost}}, \left(\frac{\frac{\text{units}}{\$ \text{ million}}}{\$ \text{ million}}\right)$	-1.26×10^{-2}	-1.42×10^{-2}	-1.11×10^{-2}	-1.04×10^{-2}	-1.82×10^{-2}	-9.29×10^{-3}

[a]0–136.1 kg of redundancy.
[b]136.1–226.8 kg of redundancy.

Table 11. Characteristics of system options and their associated deltas

System option	Redundancy level	Reliability type	Reliability	Δreliability	Cost, $ million	Δcost	Mass, kg	Δmass[b] kg
IA[a]	Single[a]	–	0.90	0	1.0	0	179.4	0
IB	Double	–	0.99	+0.09	1.2	+0.2	181.5	−2.18
IIA	Single	HRL	0.69	−0.21	2.0	+1.0	41.9	+137.48
IIA	Single	TRW	0.61	−0.29	2.0	+1.0	41.9	+137.48
IIA	Single	Life test	0.27	−0.63	2.0	+1.0	41.9	+137.48
IIB	Double	HRL	0.96	+0.06	2.35	+1.35	68.0	+111.36
IIB	Double	TRW	0.95	+0.05	2.35	+1.35	68.0	+111.36
IIB	Double	Life test	0.71	−0.19	2.35	+1.35	68.0	+111.36
IIIA	Single	High-reliability capacitor	0.71	−0.19	0.95	−0.05	128.1	+51.26
IIIA	Single	Life test	0.49	−0.51	0.95	−0.05	128.1	+51.26
IIIB	Double	High-reliability capacitor	0.99	+0.09	1.30	+0.3	252.0	−72.67
IIIB	Double	Life test	0.95	+0.05	1.30	+0.03	252.0	−72.67
IVA	Single	High-reliability capacitor	0.71	−0.19	1.8	+0.8	121.6	+57.74
IVA	Single	Life test	0.50	−0.40	1.8	+0.8	121.6	+57.74
IVB	Double	High-reliability capacitor	0.98	+0.08	2.3	+1.3	212.1	−32.79
IVB	Double	Life test	0.94	+0.04	2.3	+1.3	212.1	−32.79
VA	Single	HRL	0.70	−0.20	2.6	+1.6	59.1	+120.29
VA	Single	TRW	0.62	−0.28	2.6	+1.6	59.1	+120.29
VA	Single	Life test	0.28	−0.62	2.6	+1.6	59.1	+120.29
VB	Double	HRL	0.97	+0.07	2.9	+1.9	85.5	+93.89
VB	Double	TRW	0.95	+0.05	2.9	+1.9	85.5	+93.89
VB	Double	Life test	0.71	−0.19	2.9	+1.9	85.5	+93.89

[a]Baseline system.

[b]Δmass to the spacecraft; as the subsystems become heavier the spacecraft must lose mass to remain at 680.38 kg mass, and as the subsystems become lighter then the spacecraft can add redundancy mass.

from a satellite are equal to the total cost of the program. Then the following conversion is valid:

$$\begin{pmatrix}\text{Cost effectiveness}\\ \text{difference in dollars}\end{pmatrix} = \Delta CE \left(\frac{\text{Total mission cost}}{CE_{\text{baseline}}}\right) \tag{17}$$

The results of option comparisons are presented in Fig. 24. The individual mass, cost, and reliability deltas have been combined with Eq. (16) to form one cost effectiveness delta. To obtain a feeling for the value of delta cost effectiveness, Eq. (17) can be used to convert these deltas to dollars. Cost effectiveness deltas for the system options are plotted as a function of auxiliary-propulsion system mass. The left ends of each option are single redundant systems while the heavier systems on the right of each option area are double redundant systems.

Each option presented in Fig. 24 shows an increase in cost effectiveness associated with the double redundancy system configuration. As can be seen from Fig. 24, the source of thruster reliability data can also greatly affect the results. Inert gas and hydrazine system reliabilities are based on extensive test data, and therefore only one magnitude of reliability is shown. Ion system options (II and V) are presented with three values of reliability, while the pulsed plasma system options (III and IV) are presented with two values of reliability.

Each option presented in Fig. 24 has a heavy line included along the line of "realistic" system reliability. The selection of a "realistic" system reliability of each option was subjective. For option I the heavy line in Fig. 24 is easily defined, since only one value of system reliability is presented. For option II the heavy line in Fig. 24 is for a reliability based on ion thruster life test data, since for option II the ion thruster system must perform stationkeeping and reaction wheel desaturation, which require thruster operation at least four times daily. For a 5-yr life, this leads to 5000 or more cycles of the ion thruster. The thruster is assumed to be kept "warm" with trickle power to the cathode, vaporizer, and neutralizer. Life test data for ion thrusters has been, in general, collected during steady-state operation, with very few on-off cycles. In the opinion of the author the ion thruster reliability based on life test data presented in this report is a maximum value for a system which must undergo thousands of on-off cycles as in option II. In addition, the method of axis 1 reaction wheel desaturation for option II is to turn the ion thruster on until it is hot and then turn it off. This is because the warmup time of the ion thruster is so long (10 min) that the wheel is unloaded by the time the thruster comes up to full thrust. If axis 1 is to be unloaded by vectoring of the thruster, then there will be 8 times the allocated propellant consumed, since the moment arm in axis 1 is greatly reduced when vectoring of the thruster beam is used to generate spacecraft torque. Also, to use vectoring to unload the reaction wheel, the north–south ion thrusters must be on. The north–south thrusters can fire only once a day for a period of 4–6 h about the nodal point. The axis 1 reaction wheel must be unloaded four times a day, thus requiring the north–south thrusters to be started during periods when unwanted spacecraft translation will result. For option V, the ion thruster must perform only stationkeeping functions, which will greatly lower the number of thruster on-off cycles. An ion thruster system which must operate as in option V should have a thruster reliability near that based on the TRW comparison of ion thrusters with traveling wave tubes. For the pulsed plasma options (III and IV), the high-reliability capacitor data is assumed. From the heavy lines in the option areas of Fig. 24, the system ranking is

1. Option V — double redundancy.
2. Option I — double redundancy.
3. Option II — double redundancy.
4. Option IV — double redundancy.
5. Option III — double redundancy.

The selection of a single reliability for options II, III, IV, and V was subjective, but it served as a ranking. A better way to consider the selection is to consider what types of life test data are necessary to make options II and V appear most cost effective. The shaded area in Fig. 24 corresponds to the area where options II and V are more cost effective than option I. Point A (system option II) in Fig. 24 corresponds to a thruster and power conditioning reliability of 0.79 for 10,000 h of operation and 5000 on-off cycles. This reliability corresponds to four life tests of ion thrusters, each for 8000 h and 10,000 on-off cycles with a maximum of one system failure. Point B (system option V) in Fig. 24 corresponds to a thruster and power conditioning reliability of 0.82 for 10,000 h and 1000 on-off cycles. This reliability corresponds to four life tests of ion thrusters, each for 8000 h, and 2500 on-off cycles with a maximum of one system failure. The life tests required to obtain the system reliabilities of Points A and B, if performed successfully, will make the ion propulsion options the most cost effective.

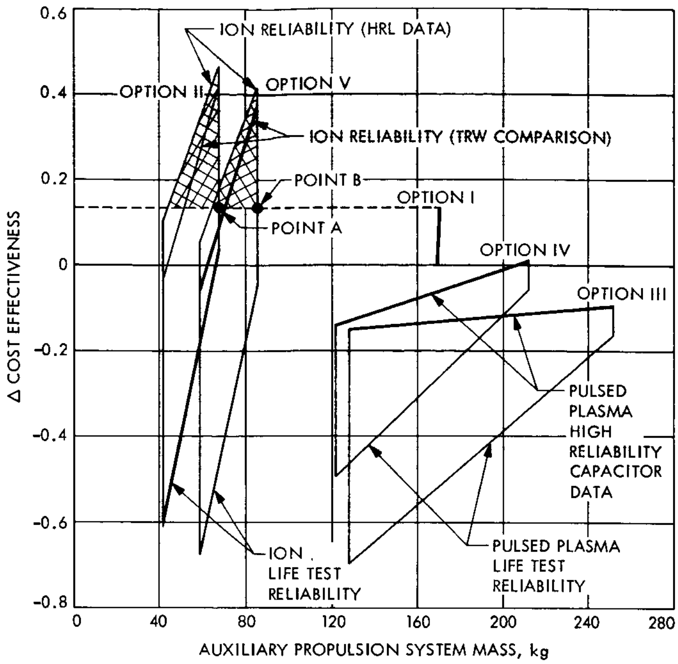

Fig. 24. Cost effectiveness comparison of system options

C. Sensitivity of Comparison to Mission Assumptions

In order to study the sensitivity of the comparisons to mission assumptions, the calculations were repeated for a new set of mission data. In order to consider each mission assumption separately, all other assumptions were held constant. In addition, only one value of subsystem reliability for the system options was used. For option I, only one reliability was assumed; for the ion system in option II, a life test data based on reliability was used; option III has been omitted from the sensitivity analysis; the high-reliability capacitor data was used for the pulsed plasma system in option IV; and the ion thruster reliability based on the TRW traveling wave tube and ion thruster comparison was used for option V.

Two new worth assumptions were given in Fig. 1, with the effect of these new mission worth curves on the influence coefficients depicted in Table 10. The system comparison calculations were repeated for the two new mission worth assumptions and are presented in Fig. 25. The net result of modified mission worth is to amplify the cost effectiveness numbers. Positive delta cost effectiveness values were increased with an increased mission worth curve, while negative delta cost effectiveness values became more negative with increased mission worth. The greater the delta cost effectiveness, the greater the amplification due to modified mission worth. The net effect of these amplifications due to increased mission worth was to spread the results out, although it did not change the ranking. For a decreased mission worth, the results came closer to the baseline cost effectiveness (the delta cost effectiveness decreased), but again, the ranking of the system options is unchanged. Therefore, for this comparison, the mission worth does not alter the final system selection.

Two new values of total program cost were assumed—$100 million and $140 million. The effect of these new total mission costs on the "influence coefficients" was depicted in Table 10. The system comparison calculations were repeated for the two new mission-worth assumptions and are presented in Fig. 26. The result of modified mission worth is to amplify the cost effectiveness numbers, as was done for modified mission worth. A decreased mission cost will increase cost effectiveness deltas, while increased mission cost will decrease cost effectiveness deltas. Again as before, the greater the delta cost effectiveness, the greater the sensitivity of the values to changes in total program cost. For this system comparison, the total mission cost does not alter the final system ranking.

A new mission probability of success given in Fig. 3 was assumed. The effect of this new curve on the "influence coefficients" is presented in Table 10. The system comparison calculations were repeated for the new mission probability of success and are presented in Fig. 27. The results are sensitive to a change in mission probability of success. The reason for this is that the mission probability of success relates reliability to mass. The large reliability and mass differences between systems can result in rather large changes in results if the "influence coefficients" are greatly changed as they are for a new curve of probability of success. The result of the new probability of success is to make the value of decreased subsystem mass greater, since the mass savings can go further toward increasing spacecraft reliability through the addition of redundancy to other subsystems. For auxiliary-propulsion subsystem mass below the 179.2-kg baseline system mass, the new probability of success calculations will shift the delta cost effectiveness curves upward on Fig. 27 for options II and V. For option IV, the effect of a new probability of success is to increase the cost effectiveness of the single system and to decrease the cost-effectiveness of the double system, since the single system mass is below 224.5 kg while the double system was above 224.5 kg.

The system ranking is affected by mission probability of success, as shown in Fig. 27. Therefore, this sensitivity

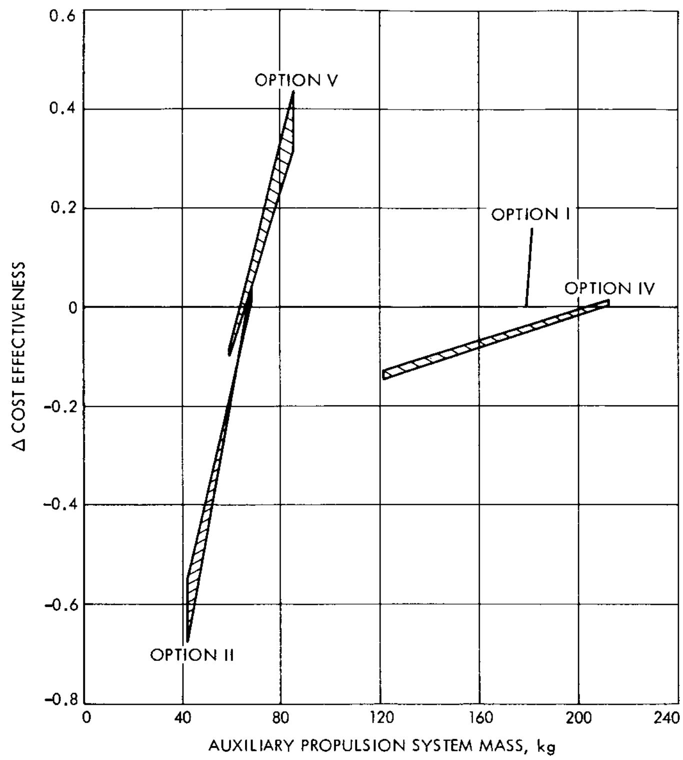

Fig. 25. Sensitivity of cost effectiveness comparisons to mission worth

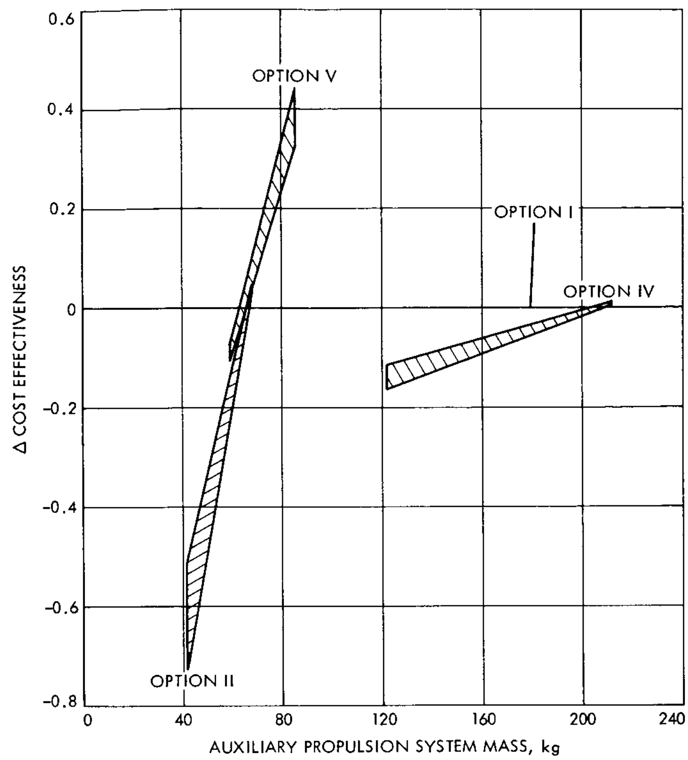

Fig. 26. Sensitivity of cost effectiveness comparisons to total mission cost

analysis has served to identify the most sensitive mission assumption. A more detailed discussion of the two mission probability of success curves was given in Section II. The justification for the use of the baseline probability of success curve is that the modified probability of success is representative of an extremely unreliable spacecraft and was presented in order to display the sensitivity of the results to modified mission probability of success.

VII. Conclusions

Using ATS-H as a sample mission, a comparison of five auxiliary propulsion systems was made. This comparison has served as one more example of the usefulness of cost effectiveness techniques as a comparison tool, especially when coupled with a study of the sensitivity of the results to mission requirements and assumptions as presented. Subsystem reliability, particularly ion thruster reliability, was shown to greatly affect the results. If specific inputs are preferred to those presented in this report, then the application of these new system inputs is strongly encouraged. It is felt that this report and Refs. 1 and 2 have provided a useful tradeoff technique which can be applied to any auxiliary-propulsion system selection.

The analysis has provided several interesting and noteworthy results. The attitude propulsion tradeoff results in the following system ranking:

1. An ion bombardment system with a hydrazine system (option V), double redundancy.
2. A monopropellant hydrazine system (option I), double redundancy.
3. An ion bombardment system with an inert gas system (option II), double redundancy.
4. A pulsed plasma system with a hydrazine system (option IV), double redundancy.
5. A pulsed plasma system with an inert gas system (option III), double redundancy.

Uncertainty in ion thruster reliability can make option V more or less favorable than option I. For example, an ion thruster reliability of 0.82 makes option V more desirable than option I. However, demonstration of an ion thruster reliability of 0.82 for option V would require a life test of four ion thrusters each for 8000 h and 2500 on-off cycles with a maximum of one system failure. It is the opinion of the author that this can be

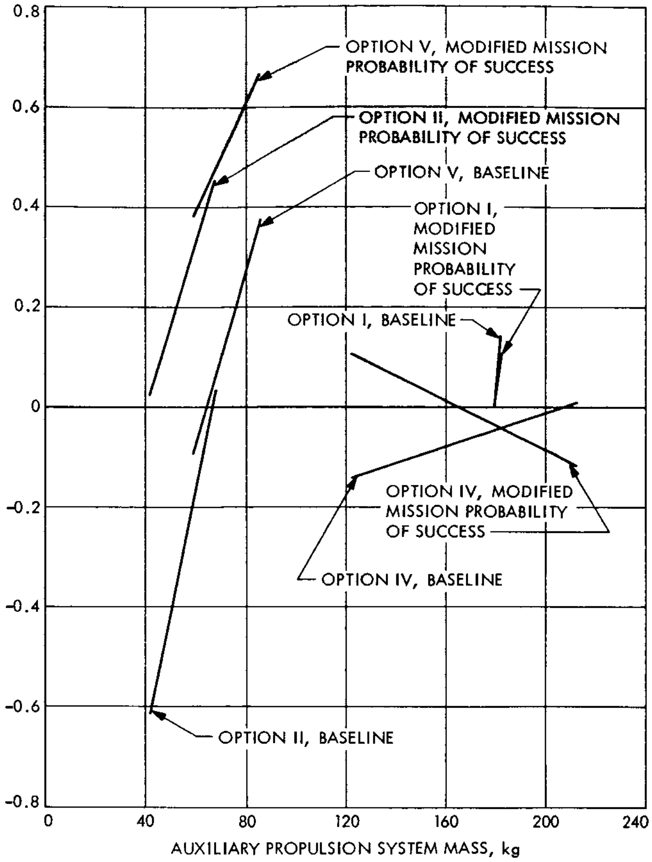

Fig. 27. Sensitivity of cost effectiveness comparisons to mission probability of success

demonstrated. But without this test data, there is a risk associated with the selection of an ion thruster system for the ATS-H spacecraft. An interesting observation from Fig. 24 is the system mass increase when shifting from single to double redundancy. The propulsion system types differ greatly in their mass increases to shift from single to double redundancy. The propulsion system types, ranked in order of lowest required mass increase to achieve higher system redundancy, are:

1. Hydrazine systems (option I).
2. Ion systems (options II, V)
3. Pulsed plasma (options III, IV)

As can be seen, the heavy system mass for the double pulsed plasma system greatly penalizes options III and IV. This is due to the requirement of doubling propellant and capacitor mass to achieve double system reliability. With the improvement of capacitor specific mass to 44.1 or 66.1 J/kg (for high reliability at 10^7 discharges), the mass of pulsed plasma systems and the mass difference between single and double redundant systems should be decreased.

There were no reaction wheels for option III, and the associated cost, mass, and reliability changes for the removal of the reaction wheels have been incorporated into this study. The main reason for the high mass of option III was the uncertainty of the direction of spacecraft disturbance torques, which required that some additional propellant be carried by both plus and minus torque thrusters. The high mass of option III is the primary reason for its low ranking. On other missions, with different mission assumptions, the operation of a pulsed plasma system in a limit cycle mode without reaction wheels may be favorable. But for this mission and the assumed system inputs, option III was the least favorable.

Triply redundant systems were not studied in Ref. 1; however, triply redundant systems for option V and I were calculated (Fig. 28). It appears that a triply redundant system improves the ranking of option V and lowers the ranking of option I. This result is included to show how cost effectiveness techniques can be used to select the proper system redundancy level.

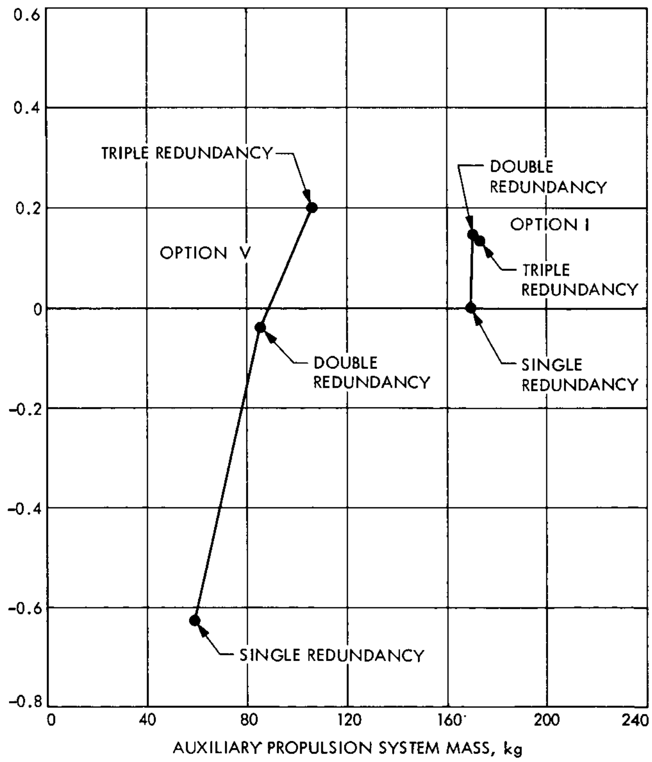

Fig. 28. The effect of triple redundancy on options I and V

The results of the sensitivity analysis were to identify the mission probability of success as the mission variable which most strongly alters the result. This is the one mission assumption that must be justified most strongly by the satellite system analyst. The example mission probability of success curve was selected from past experience with representative data. If other mission probability of success curves are preferred, then the use of these new curves is strongly encouraged.

VIII. Recommendations

The ion options II and V were found to have a region of favorability over the hydrazine option I system. The ion thruster reliability in this region is, in general, above what has presently been demonstrated. Ion thruster life tests are highly recommended, since successful life tests will remove the risk presently associated with the selection of these propulsion systems for long-life spacecraft. In addition, the continued development and flight qualification of mercury and cesium ion thrusters in the 1.33- to 8.90-mN-thrust range will lower the cost of these devices and make them more attractive for this application.

Hydrazine option I is found to be most favorable when present life test data for ion thrusters was assumed. The hydrazine system has seen extensive use on spacecraft in the past and this will continue. The use of hydrazine systems should provide a gradual decrease in system cost as a wider array of flight-qualified hardware is developed. The compilation of recent ground and space test data should be performed as recent hydrazine components provide more reliable operation. In addition, a better understanding of thruster "cold" and "warm" start life characteristics is warranted, since without a complete understanding of this phenomenon hydrazine propulsion system reliability is not fully understood.

The pulsed plasma options were the least favorable for this mission. The long-life characteristics of these thrusters and the multistart nature of their operation make them attractive for the ATS-H spacecraft mission. However, the capacitor mass for these devices strongly penalizes them. The single most important recommendation for pulsed plasma systems for long-life north–south stationkeeping is the development, test, and flight qualification of a capacitor with a specific mass of 44.1–66.1 J/kg with a reliability of 0.98 for 10^7 pulses.

Nomenclature

a orbit semimajor axis, m

A_{dr} ρ_d/ρ_{ds}

A_p projected surface area, m^2

A_{sp} area of solar panels, m^2

CE cost effectiveness, units /$ million

$CE_{baseline}$ baseline cost effectiveness, units/$ million

C_i mission cost ($ million) where $\sum_i C_i$ = total mission cost

F thrust, N

F_{solar} solar pressure force, N

g_c constant of proportionality in Newton's second law

$I_{1,2,3}$ moment of inertia about 1, 2, or 3 axis, kg m^2

I_{sp} specific impulse, N-s/kg

K gravitational constant for earth = 3.99×10^{14} N-m^2/kg

$K_{I/C}$ incident radiant flux/velocity of light = 454.85×10^{-8} N/m^2

L center of pressure/center of gravity offset, m

l thruster moment arm, m

M_f final spacecraft mass after depletion of propellant, kg

M_p mass of propellant, kg

M_0 initial spacecraft mass, kg

P_i mission probability of success, where i refers to a time increment

P_s solar pressure, N/m^2

T torque, N-m

$T_{(1)(2)(3)}$ torque about the 1, 2, or 3 axis; for this spacecraft these axes coincide with the yaw, pitch, and roll axes, N-m

t time, s

W_i worth of mission, where i refers to a time increment, units

Δcost difference in comparative subsystem cost and the baseline subsystem cost, where increases in cost above baseline cost are positive, $ million

Δmass difference in baseline subsystem mass and comparative subsystem mass, where increases in mass above baseline mass are negative, kg

Δreliability difference in comparative subsystem reliability and the baseline subsystem reliability, where increases in reliability above baseline reliability are positive

$\frac{\Delta CE}{\Delta \text{cost}}$ cost influence coefficient, (units/$ million)/ $ million

$\frac{\Delta CE}{\Delta \text{mass}}$ mass influence coefficient, (units/$ million)/kg

$\frac{\Delta CE}{\Delta \text{reliability}}$ reliability influence coefficient, (units/ $ million)/increase in reliability

ΔV velocity change, m/s

δ, ϕ, ψ spacecraft displacement angle (Fig. 18), deg

ρ_d diffuse coefficient of reflectivity

ρ_{dr} $\rho_s + \rho_d$

ρ_s specular coefficient of reflectivity

θ sun–spacecraft angle (also sun–spacecraft surface angle), deg

$\dot{\theta}_{max}$ spacecraft angular rate, rad/s

$\dot{\theta}_s$ angle required to come to stop, rad

ω_0 mean orbital angular velocity, rad/s

English to S.I. units conversion table

To convert from	To	Multiply by
lbf	N	4.44822
lbf-s/lbm	N-s/kg	9.80665
W/mlbf	W/mN	0.22481
lbf-ft	N-m	1.35582
ft	m	0.3048
slug-ft^2	kg-m^2 (N-m-s^2)	1.35690
lbm	kg	0.45359

References

1. Holcomb, L. B., *Satellite Auxiliary-Propulsion Selection Techniques*, Technical Report 32-1505, Jet Propulsion Laboratory, Pasadena, Calif., Nov. 1, 1970.
2. Holcomb, L. B., *Satellite Auxiliary-Propulsion Selection Techniques, Addendum Survey of Auxiliary Electric Propulsion Systems*, Technical Report 32-1505, Addendum, Jet Propulsion Laboratory, Pasadena, Calif., July 15, 1971.
3. Gould, L. M., *Final Report of ATS Advanced Mission Study*, NASA, CR-120873, Contract No. NAS-3-14359, to be published.
4. Robinson, D. L., and Raymond, H. A., *Applications Technology Satellite Advanced Mission Study*, Contract No. NAS-3-14360, Monthly Progress Report, Vol. I, II, and III, May 1971.
5. Fleischer, G. E., "A Pulsed Plasma Jet Attitude Controller for an ATS-H Synchronous Satellite," Internal Document, Engineering Memo 344-365ATS, Jet Propulsion Laboratory, Pasadena, Calif., Dec. 1971.
6. *Spacecraft Radiation Torques*, NASA Space Vehicle Design Criteria, NASA SP-8027, Oct. 1969.
7. *Spacecraft Gravitational Torques*, NASA Space Vehicle Design Criteria, NASA SP-8024, May 1969.
8. *Spacecraft Aerodynamic Torques*, NASA Space Vehicle Design Criteria, NASA SP-8058, Jan. 1971.
9. *Spacecraft Magnetic Torques*, NASA Space Vehicle Design Criteria, NASA SP-8018, Mar. 1969.
10. Kaplan, M. H., "All-Electric Thruster Control of a Geostationary Communications Satellite Which Employs Narrow-Beam Antennas," AIAA Paper 72-436, AIAA 9th Electric Propulsion Conference, Bethesda, Md., Apr. 1972.
11. Isley, W. C., and Duck, K. I., "Propulsion Requirements for Communications Satellites," AIAA Paper 72-515, Proceedings of AIAA Fourth Communications Satellite Systems Conference, Washington, D. C., Apr. 1972.
12. Benson, R. A., "Earth Orbital Mission Requirements for Secondary Propulsion Systems and Their Impact on Colloid Systems," ASME Paper 70-Av/SpT-31, Space Technology and Heat Transfer Conference, Los Angeles, Calif., June 1970.
13. *Electric Propulsion Reliability Analysis*, NASA Contract NAS7-559, Hughes Aircraft Co., (R&D Div.), Culver City, Calif., unpublished report.
14. *Feasibility Study for a Multi-Mission Electric Propulsion Spacecraft*, Report 18305-6001-R000, Contract No. NAS-2-6287, TRW Systems, One Space Park, Redondo Beach, Calif., June 1971.
15. Earles, D. R., and Eddins, M. F., *Reliability Engineering Data Series Failure Rates*, Avco Corporation, Wilmington, Mass., Apr. 1962.

NASA — JPL — Coml., L.A., Calif.